

**2018 Spring**

**“Advanced Physical Metallurgy”  
- Bulk Metallic Glasses -**

**04.18.2018**

**Eun Soo Park**

**Office: 33-313**

**Telephone: 880-7221**

**Email: [espark@snu.ac.kr](mailto:espark@snu.ac.kr)**

**Office hours: by appointment**

# 4 *Synthesis of Bulk Metallic Glasses*

**Metallic glasses:** produced by rapidly solidifying metallic melts to cooling rate **about  $10^6$  K/s**



**BMG :** Produced by relatively slow solidification rates of **about  $10^3$  K/s or less**

## 4.2 Principles of Rapid Solidification Processing: Huge departure from equilibrium

- 1) A small quantity of the molten metal is ejected using a shock wave on to a conducting substrate. The molten metal spreads in the form of a thin layer, typically a few tens of micrometers (but usually about 20-50  $\mu$ m) in thickness, and the heat is extracted rapidly by conducting copper substrate.
- 2) Basic requirements to achieve high solidification rates:
  - a. Forming a thin layer (film or ribbon) of the molten metal
  - b. Intimate thermal contact with a good heat-conducting substrate to rapidly extract the heat from the liquid metal

3)

$$R = \frac{A}{x^2}$$

where

$x$  is the distance from the splat/substrate interface

the constant  $A$  is a function of the material properties and initial temperatures, but is independent of  $x$

The value of  $A$  is  $8.1 \times 10^{-3} \text{ m}^2 \text{ K s}^{-1}$  for ideal cooling (when the heat transfer coefficient is  $\infty$ ) and it is less for nonideal cooling conditions. For example, assuming an average value of  $A = 10^{-3} \text{ m}^2 \text{ K s}^{-1}$ , for rough estimates, the solidification rate achieved will be approximately  $10^5 \text{ K s}^{-1}$  for  $x = 100 \mu\text{m}$  and  $10^9 \text{ K s}^{-1}$  for  $x = 1 \mu\text{m}$ . The typical thickness of a rapidly solidified foil is about  $50 \mu\text{m}$ , and therefore the foil would have solidified at a rate of approximately  $10^6 \text{ K s}^{-1}$ . These examples serve to illustrate that it is necessary to have as small a section thickness as possible to achieve high solidification rates.

### 4.3 General Techniques to Achieve High Rates of Solidification

“Energize and quench” – increase the free energy of the system (by either raising the temperature, or pressure or the input of mechanical energy, or by other means) and subsequently quenching the material to either retain the metastable phase or to use it as an intermediate step to achieve the desired microstructure and/or properties → Some very interesting properties

**4.4 Melt Spinning:** the most commonly used method to produce long and continuous rapidly solidified ribbons, wires, and filaments

- Free flight melt-spinning, Chill block melt-spinning  
: a small quantity of the alloy is melted inside a crucible or by levitation methods, and then ejected by pressurization through a fine nozzle onto a fast-rotating copper wheel.

- **Crucible material:** based on its chemical compatibility with the melts, its temperature handling capability, its resistance to thermal shock, its low thermal conductivity, and its low porosity (e.g., dense alumina and quartz)

- **Nozzle:** about 50  $\mu\text{m}$  to 1250  $\mu\text{m}$ , alumina, graphite, SiC, Sapphire, and pyrex glass

- **Ejection pressures:** 5-70 kPa depending on desired melt delivery rate, high ejection pressures → improvement of the wetting pattern and better thermal contact between the melt puddle and the substrate.

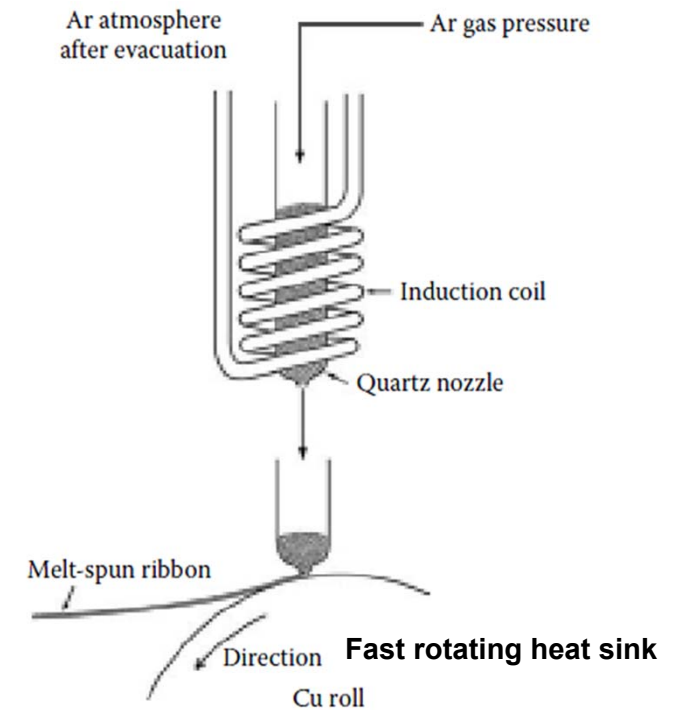


FIGURE 4.1  
Schematic illustration of the melt-spinning process.

#### 4.4 Melt Spinning: the most commonly used method to produce long and continuous rapidly solidified ribbons, wires, and filaments

##### - Wheel for melt-spinning:

- a) extract the heat from the ribbon as quickly as possible
- b) a variety of materials including copper, stainless steel, chromium, and molybdenum
- c) outer surface of the wheel is generally polished to remove any surface roughness  
due to wheel side of the cast ribbon → almost an exact replica of the wheel surface
- d) Wheel speed is an important parameter in determining the thickness of the ribbon  
ex\_  $\text{Fe}_{40}\text{Ni}_{40}\text{B}_{20}$  alloy, 250 mm diameter copper wheel,  
substrate velocity o 26.6 m/s → 37  $\mu\text{m}$ , substrate velocity o 46.5 m/s → 22  $\mu\text{m}$ ,

- **Operation:** carried out in vacuum, air, or inert atmosphere, or reactive gas depending on the chemical and physical properties of the charge

- **Solidification rate:** typically about  $10^5$ - $10^6$  K/s,

- **Typical dimensions of ribbons:** 2-5 mm → can be increased using the planar flow casting method

- **Thickness:** 20-50  $\mu\text{m}$  → cannot be increased

➡ These thin ribbon used to measure the thermal properties ( $T_g$ ,  $T_x$ , and  $T_l$ ) using the DSC and or DTA methods. This is appropriate because the thermal properties of the glass do not depend on the dimensions of the glass specimen (in general). → **Calculation of GFA parameters**

## 4.5 Bulk Metallic Glass

### \* History of Metallic Glasses

- First amorphous metal produced by evaporation in 1934.

*\* j. Kramer, Annalen der Phys. 1934; 19: 37.*

- First amorphous alloy (CoP or NiP alloy)  
produced by electro-deposition in 1950.

*\* A. Brenner, D.E. Couch, E.K. Williams, J. Res. Nat. Bur. Stand. 1950: 44; 109.*

- First metallic glass ( $\text{Au}_{80}\text{Si}_{20}$ )  
produced by splat quenching at Caltech by Pol Duwez in 1957.

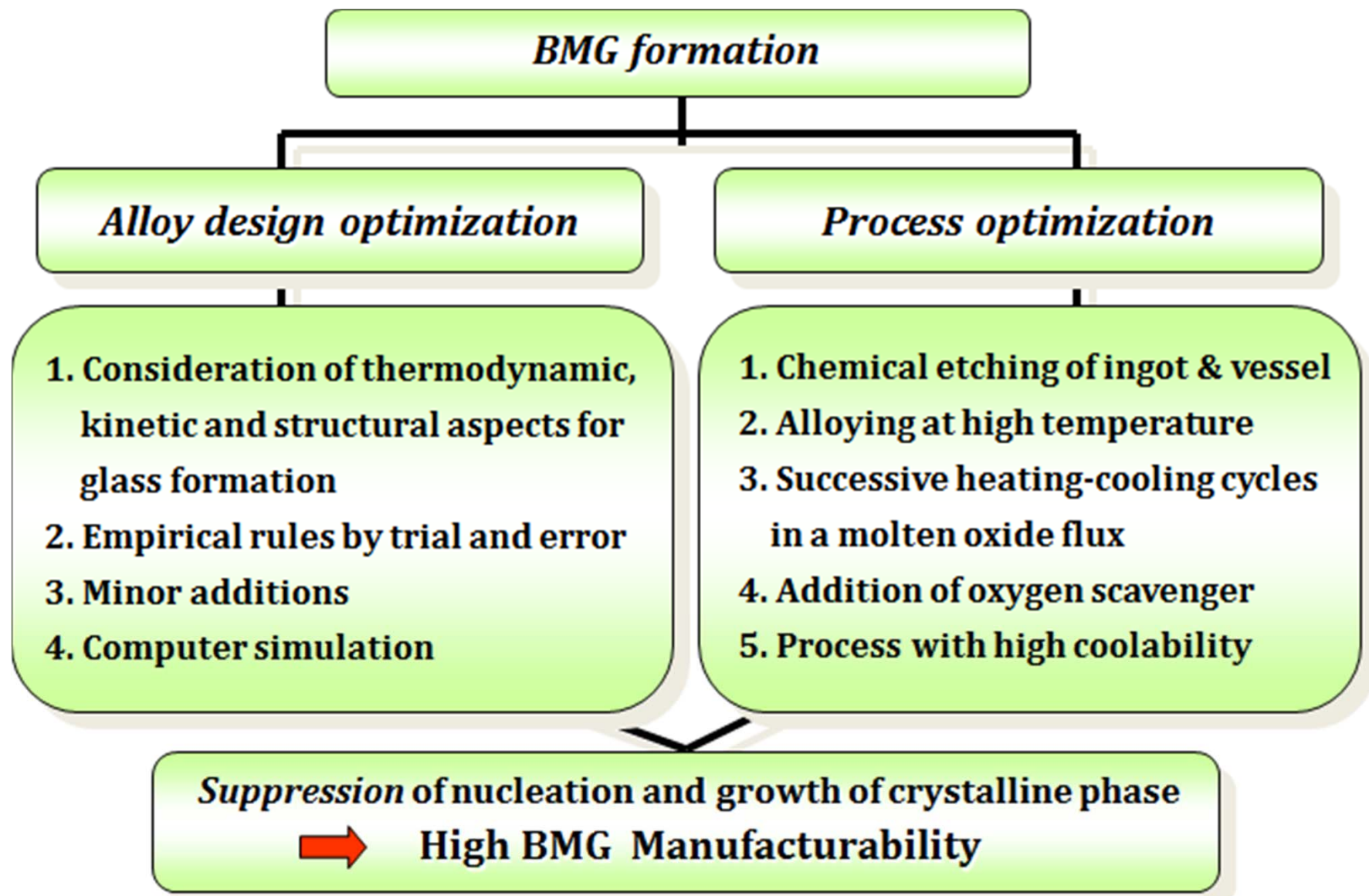
*\* W. Klement, R.H. Willens, P. Duwez, Nature 1960; 187: 869.*

- First **bulk metallic glass** ( $\text{Pd}_{77.5}\text{Cu}_6\text{Si}_{16.5}$ )  
produced by droplet quenching at Harvard Univ.  
by **H.S. Chen and D. Turnbull** in 1969

*\* H.S. Chen and D. Turnbull, Acta Metall. 1969; 17: 1021.*

produced by water quenching of PdTMSi, Pt-Ni-P and Pd-Ni-P system  
by **H.S. Chen** in 1974 ( long glassy rods, 1-3 mm in diameter and several centimeters in length)

*\* H.S. Chen, Acta Metall. 1974; 22: 1505*



## 4.6 Bulk Metallic Glass Casting Methods

**4.6.1 Water-Quenching Method** : simplest of the quenching methods used for centuries to harden steel (by transforming the soft austenite to the hard martensite phase)

- **Cooling rate: about 10-100 K/s**, inherently dependent on the heat transfer efficiency of quenching medium, the size of the specimen, and its heat transfer properties.
- A distinct advantage of the water-quenching method is that due to the slow solidification rates, the cast specimen **contains much less residual stresses and porosity**.

The world's biggest glassy alloy ever made

*Intermetallics* 30 (2012) 19–24

Nobuyuki Nishiyama<sup>a,\*</sup>, Kana Takenaka<sup>a</sup>, Haruko Miura<sup>a</sup>, Noriko Saidoh<sup>a</sup>, Yuqiao Zeng<sup>b</sup>, Akihisa Inoue<sup>b</sup>

<sup>a</sup>RIMCOF Tohoku Univ. Lab., The Materials Process Technology Center, Sendai 980-8577, Japan

<sup>b</sup>Institute for Materials Research, Tohoku University, Sendai 980-8577, Japan

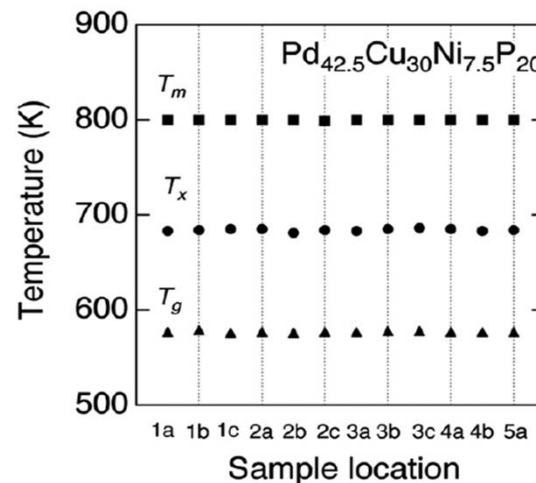
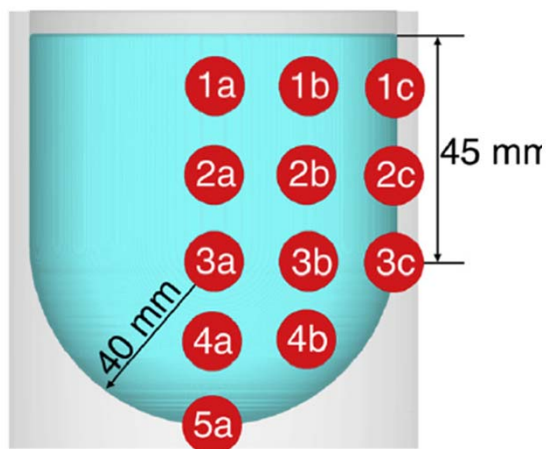


**TABLE 4.2**

Details of Bulk Metallic Glassy Rods Produced by the Water Quenching Method

Alloy System	Diameter of the Rod (mm)	Critical Cooling Rate (K s <sup>-1</sup> )	Year	Reference
(Pd <sub>1-x</sub> M <sub>x</sub> ) <sub>0.835</sub> Si <sub>0.165</sub>	1–3	<10 <sup>3</sup>	1974	[18]
(Pd <sub>1-x</sub> T <sub>x</sub> ) <sub>1-x</sub> P <sub>x</sub> P	1–3	<10 <sup>3</sup>	1974	[18]
(Pt <sub>1-x</sub> Ni <sub>x</sub> ) <sub>1-x</sub> P <sub>x</sub> P	1–3	<10 <sup>3</sup>	1974	[18]
Pd <sub>40</sub> Ni <sub>40</sub> P <sub>20</sub>	5–6	~1	1982	[20]
Pd <sub>40</sub> Ni <sub>40</sub> P <sub>20</sub> (flux treated)	10		1984	[21]
Zr <sub>65</sub> Al <sub>7.5</sub> Ni <sub>10</sub> Cu <sub>17.5</sub>	<16	1.5	1993	[37]
Zr <sub>41.2</sub> Ti <sub>13.8</sub> Cu <sub>12.5</sub> Ni <sub>10</sub> Be <sub>22.5</sub>	14	<10	1993	[25]
Pd <sub>40</sub> Cu <sub>30</sub> Ni <sub>10</sub> P <sub>20</sub>	40	1.57	1996	[26]
Pd <sub>40</sub> Cu <sub>30</sub> Ni <sub>10</sub> P <sub>20</sub> (flux treated)	50–72	0.1	1997	[19]
Pd <sub>40</sub> Ni <sub>40</sub> P <sub>20</sub>	7	100	1999	[38]
Pd <sub>40</sub> Ni <sub>32.5</sub> Fe <sub>7.5</sub> P <sub>20</sub>	7	100	1999	[38]
Pd <sub>40</sub> Ni <sub>20</sub> Fe <sub>20</sub> P <sub>20</sub>	7	100	1999	[38]
Mg <sub>65</sub> Y <sub>10</sub> Cu <sub>15</sub> Ag <sub>5</sub> Pd <sub>5</sub>	12		2001	[39]
Y <sub>56</sub> Al <sub>24</sub> Co <sub>20</sub>	1.5		2003	[40]
Y <sub>36</sub> Sc <sub>20</sub> Al <sub>24</sub> Co <sub>20</sub>	25		2003	[40]
Pt <sub>60</sub> Cu <sub>20</sub> P <sub>20</sub>	<4		2004	[41]
Pt <sub>60</sub> Cu <sub>16</sub> Co <sub>2</sub> P <sub>22</sub> (flux treated)	16		2004	[41]
Pt <sub>57.5</sub> Cu <sub>14.7</sub> Ni <sub>5.3</sub> P <sub>22.5</sub> (flux treated)	16		2004	[41]
Pt <sub>42.5</sub> Cu <sub>27</sub> Ni <sub>9.5</sub> P <sub>21</sub> (flux treated)	20		2004	[41]

Most common container material: Quartz but compatibility between melt and the crucible \_important issue For MG BMG, when a quartz tube was used, Si dissolved in the Mg melt as an impurity and acted as heterogeneous nucleation sites. Consequently, the GFA of the alloy was reduced. On the other hand, when an iron tube was used, there was no interaction between iron and the Mg-melt. → D<sub>max</sub> = 12 mm



## 4.6 Bulk Metallic Glass Casting Methods

### 4.6.2 High-Pressure Die Casting

: offer high solidification rates (because heat is extracted more rapidly by the metal mold due to good contact), high productivity, low casting defect, and possible to produce more complex shapes even in alloys with a high viscosity

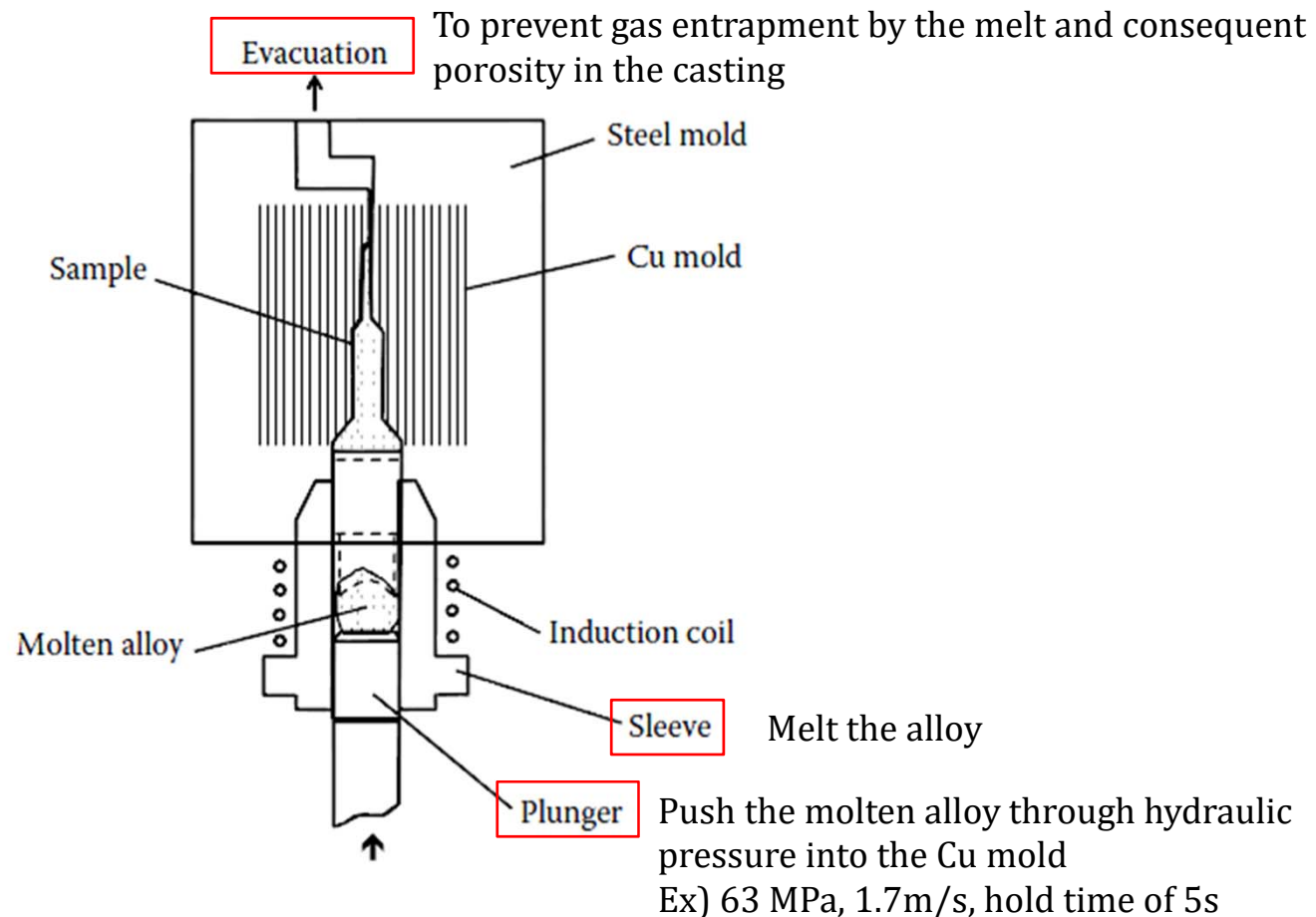
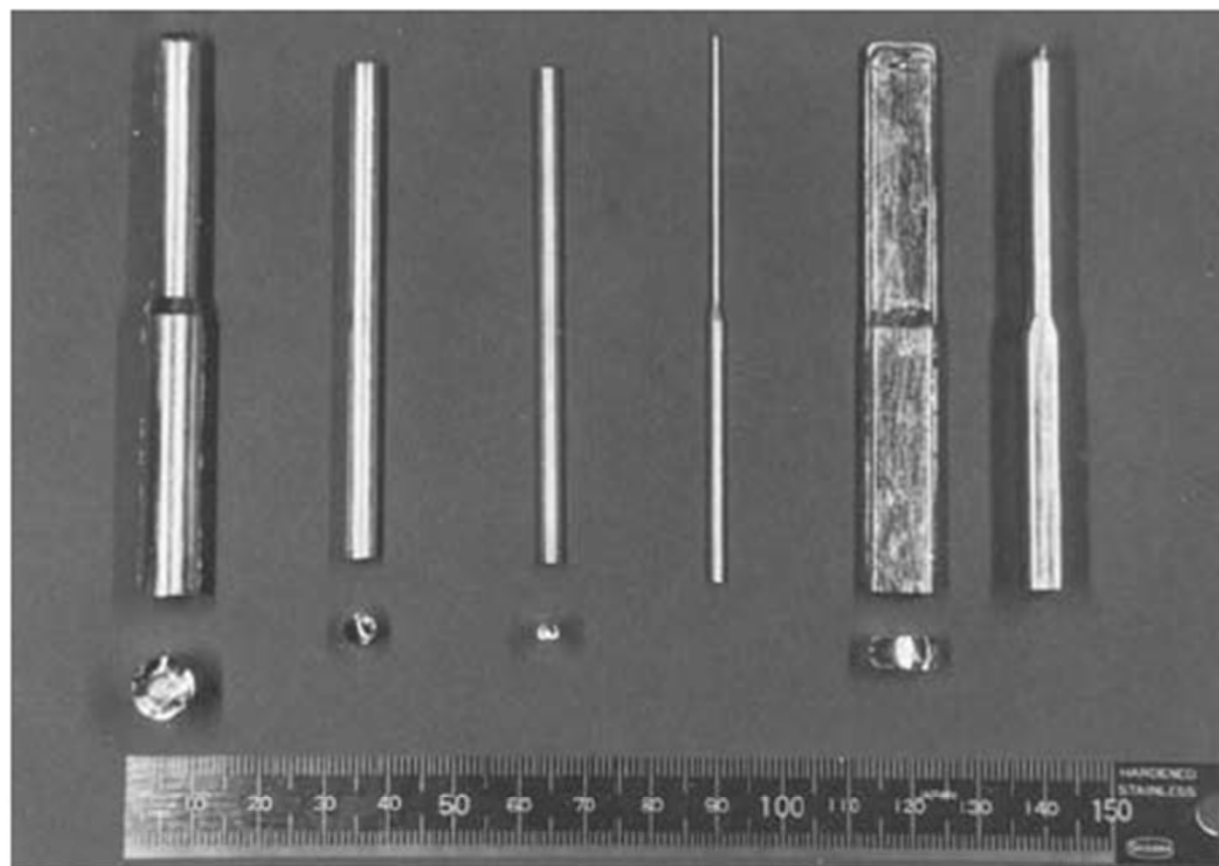


FIGURE 4.5

Schematic diagram of the high-pressure die casting equipment designed and used by Inoue et al. (Reprinted from Inoue, A. et al., *Mater. Trans., JIM*, 33, 937, 1992. With permission.)



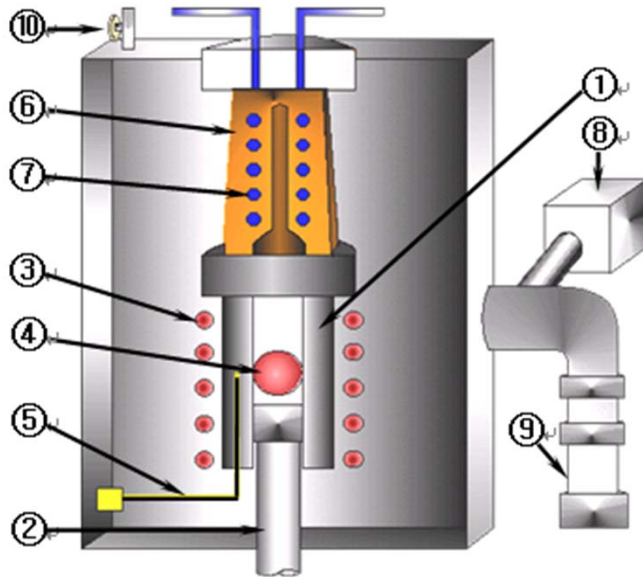
**FIGURE 4.6**

Photographs of the  $\text{Mg}_{65}\text{Cu}_{25}\text{Y}_{10}$  rods and sheets (of different diameters) produced by the high-pressure die-casting technique. The length of the samples is 80 mm and the thickness or diameter varies from 0.5 to 9 mm. Note the bright and shiny appearance of both the types of samples. (Reprinted from Inoue, A. et al., *Mater. Trans., JIM*, 33, 937, 1992. With permission.)

## 4.6 Bulk Metallic Glass Casting Methods

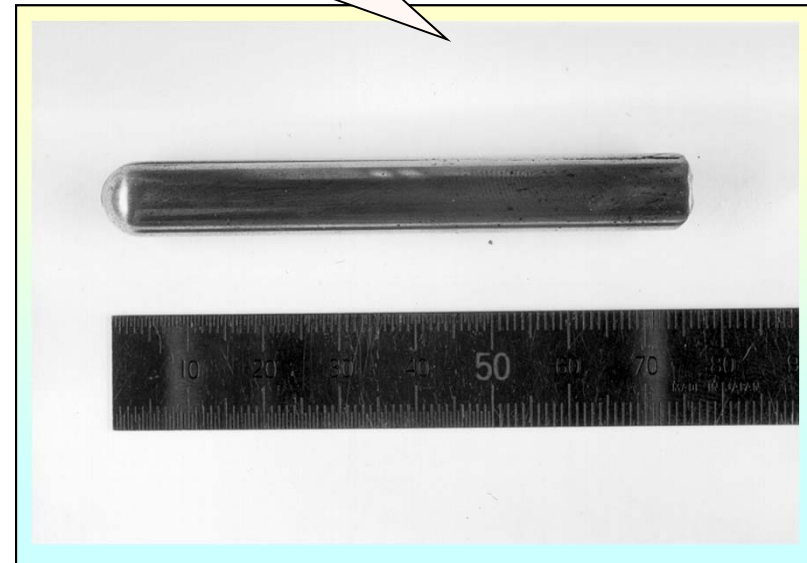
### 4.6.6 Squeeze-casting Method

: involves solidification of the molten metal under a high pressure within a closed die by utilizing a hydraulic pressure → Net-shape forming capability, fully dense sample



①	Graphite crucible	⑥	Copper mold
②	Plunger	⑦	Water cooling
③	Induction coil	⑧	Rotary pump
④	Molten alloy	⑨	Diffusion pump
⑤	Thermocouple	⑩	Evacuation valve

Squeeze Casting  
10mm



Push the molten alloy through hydraulic pressure into the Cu mold  
Ex) 100 MPa, hold time of 2min until the liquid alloy completely solidified

→ Undercooling to much below the equilibrium solidification temperature

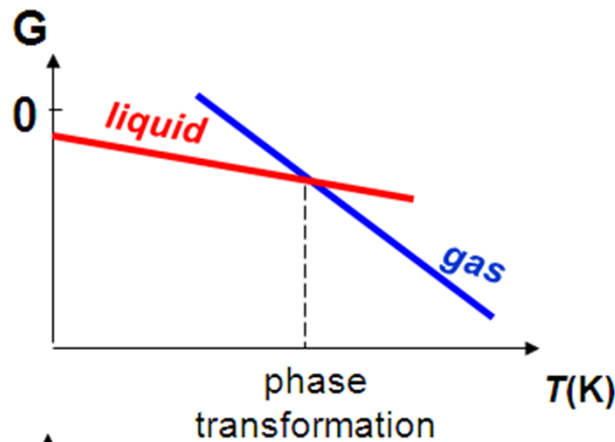
# Gibbs Free Energy as a Function of Temp. or Pressure

Considering P, T  $G = G(T, P)$

$$dG = VdP - SdT$$

$$G(P, T) = G(P_0, T_0) + \int_{P_0}^{P_1} V(T_0, P)dP - \int_{T_0}^{T_1} S(P, T)dT$$

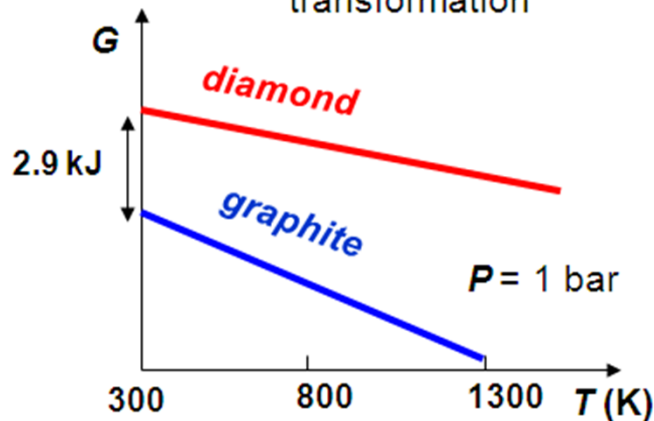
## 1) Temperature Effects



$$S(\text{water}) = 70 \text{ J/K}$$

$$S(\text{vapor}) = 189 \text{ J/K}$$

$$\left( \frac{\partial G}{\partial T} \right)_P = -S$$



$$S(\text{graphite}) = 5.74 \text{ J/K},$$

$$S(\text{diamond}) = 2.38 \text{ J/K},$$

## 2) Pressure Effects

If the two phases in equilibrium have different molar volumes, the only way to maintain equilibrium at different pressures is by varying the equilibrium temperature.

If  $\alpha, \beta$  phases are equilibrium,

$$dG^\alpha = V^\alpha dP - S^\alpha dT \quad \left( \frac{dP}{dT} \right)_{eq} = \frac{S^\beta - S^\alpha}{V^\beta - V^\alpha} = \frac{\Delta S}{\Delta V}$$

$$dG^\beta = V^\beta dP - S^\beta dT \quad \text{where, } \Delta S = \frac{\Delta H}{T_{eq}}$$

At equilibrium,

$$dG^\alpha = dG^\beta$$

$$\left( \frac{dP}{dT} \right)_{eq} = \frac{\Delta H}{T_{eq} \Delta V}$$

**: Clausius-Clapeyron Relation**

(applies to all coexistence curves)

On a pressure-temperature (P-T) diagram, the line separating the two phases is known as the coexistence curve. The Clausius-Clapeyron relation gives the slope of this curve.

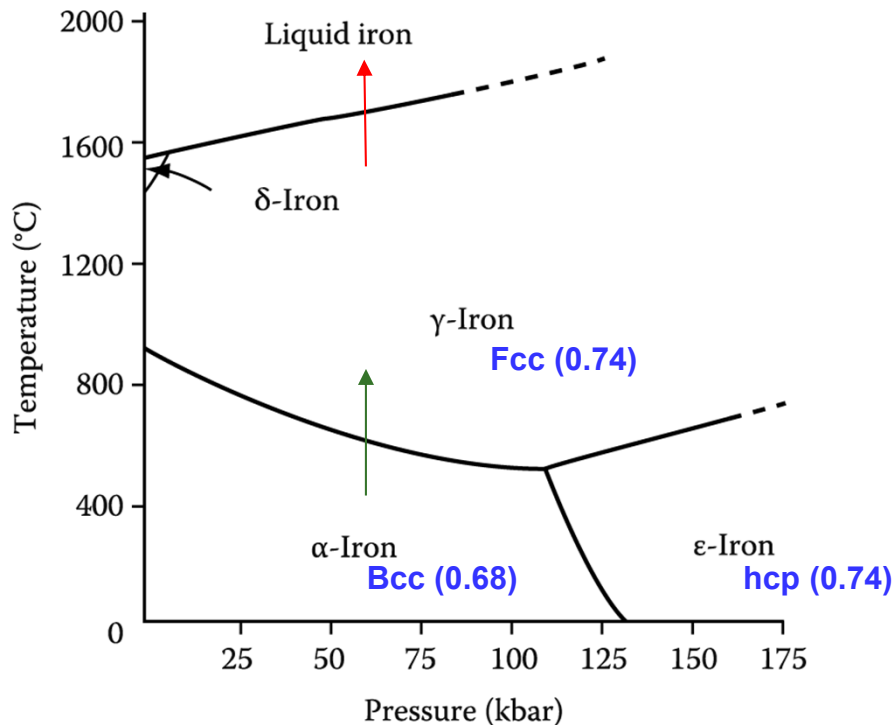


Fig. 1.5 Effect of pressure on the equilibrium phase diagram for pure iron

**Case 1.  $\gamma \rightarrow$ liquid ;  $\Delta V (+)$ ,  $\Delta H(+)$**

$$\left( \frac{dP}{dT} \right) = \frac{\Delta H}{T_{eq} \Delta V} > 0$$

**Case 2.  $\alpha \rightarrow \gamma$  ;  $\Delta V (-)$ ,  $\Delta H(+)$**

$$\left( \frac{dP}{dT} \right) = \frac{\Delta H}{T_{eq} \Delta V} < 0$$

$$\left( \frac{\partial G}{\partial P} \right)_T = V$$

**H6: Explain the role of P to improve GFA.**

## 4.6 Bulk Metallic Glass Casting Methods

### 4.6.3 Copper Mold Casting : most common and popular method to produce BMGs

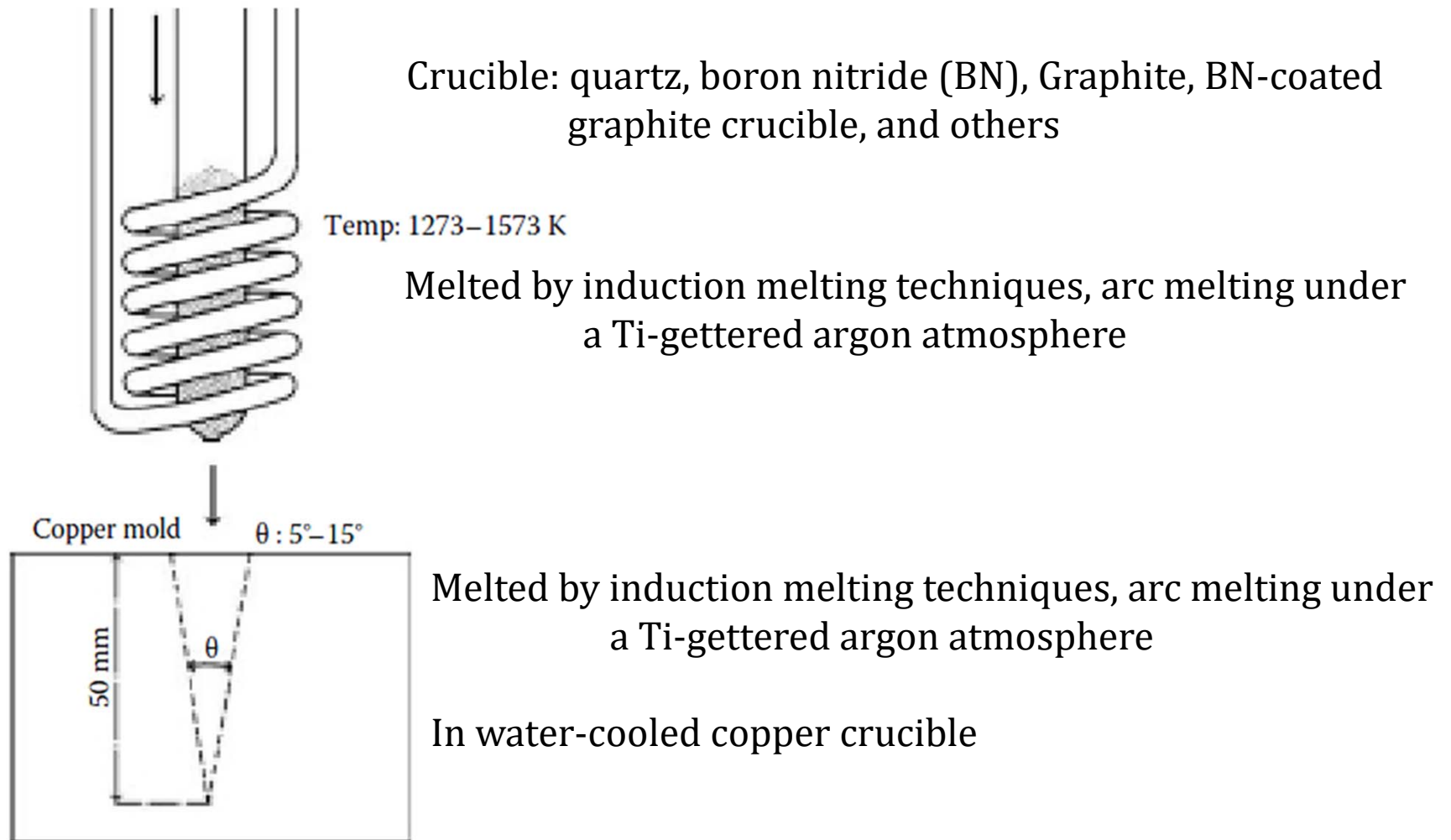


FIGURE 4.7

Schematic diagram of the equipment used to prepare bulk metallic glassy alloys by the copper mold wedge-casting technique. (Reprinted from Inoue, A. et al., *Mater. Trans., JIM*, 36, 1276, 1995. With permission.)

## 4.6 Bulk Metallic Glass Casting Methods

### 4.6.3 Copper Mold Casting

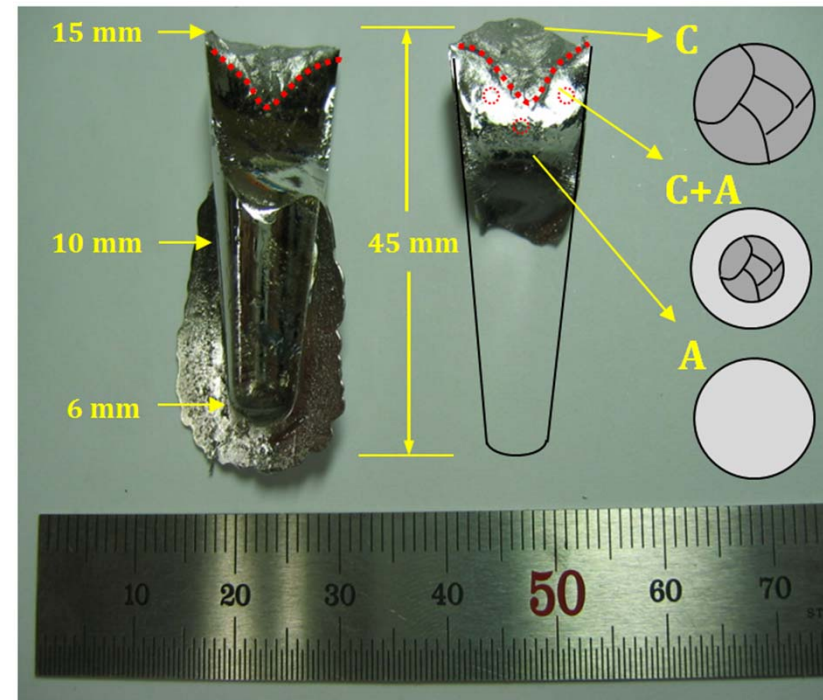
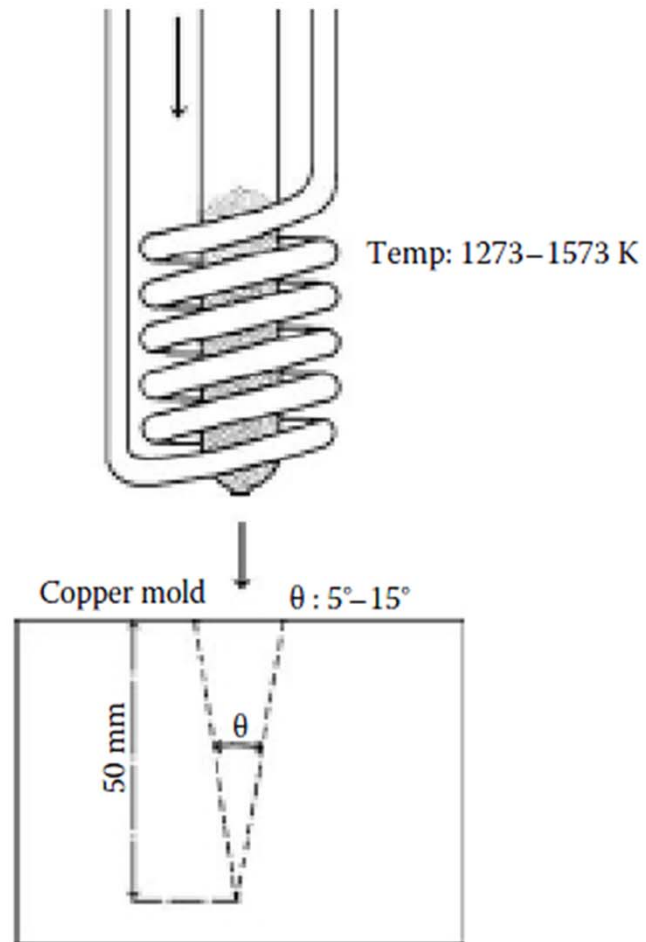


FIGURE 4.7

Schematic diagram of the equipment used to prepare bulk metallic glassy alloys by the copper mold wedge-casting technique. (Reprinted from Inoue, A. et al., *Mater. Trans., JIM*, 36, 1276, 1995. With permission.)

## Solidification Analyses of Bulky $Zr_{60}Al_{10}Ni_{10}Cu_{15}Pd_5$ Glass Produced by Casting into Wedge-Shape Copper Mold

Akihisa Inoue, Yoshiyuki Shinohara<sup>†</sup>, Yoshihiko Yokoyama and Tsuyoshi Masumoto

*Institute for Materials Research, Tohoku University, Sendai 980-77, Japan*

The liquid-crystalline transformation behavior during continuous cooling and the transformation-induced structure were examined for a  $Zr_{60}Al_{10}Ni_{10}Cu_{15}Pd_5$  molten alloy which was ejected into a wedge-shape cavity in a copper mold. The wedge-shape cavity has a constant depth of 50 mm and different vertical angles ( $\theta$ ) ranging from 5 to 15 degrees. The ejection temperature of the molten alloy was also changed in the range of 1273 to 1573 K. The cast structure consists only of a glassy phase in the  $\theta$  range smaller than 10 degrees and changes to a mixed structure consisting of glassy and non-equilibrium crystalline  $Zr_2Ni$  and  $Zr_2Cu$  phases in the higher  $\theta$  range. The glass transition temperature and crystallization temperature of the cast metal glass are 683 and 778 K, respectively, which agree with those for the melt-spun glassy ribbon. The start ( $C_s$ ) and termination ( $C_t$ ) points for the transformation from the supercooled liquid to crystalline phases during continuous cooling were determined from the thermal analytical data obtained at different sites in the wedge-shape cavity and the continuous-cooling-transformation (C.C.T.) curves were constructed. The nose temperature ( $T_n$ ) and the time ( $t_n$ ) up to the nose point in the C.C.T. curves were 1018 K and 0.93 s respectively. The critical cooling rate for glass formation defined by  $(T_n - T_c)/t_n$  is evaluated to be 110 K/s. Further, the time interval between  $C_s$  and  $C_t$  is as short as 0.2 s and the fast growth reaction is attributed to the easy formation of the non-equilibrium crystalline phases and the increase in temperature caused by the precipitation-induced recalescence.

(Received May 11, 1995)

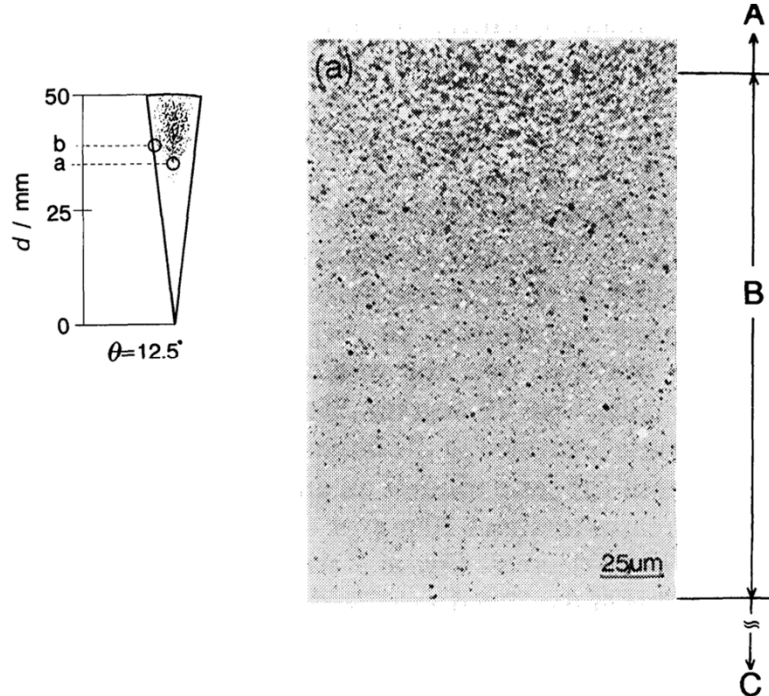
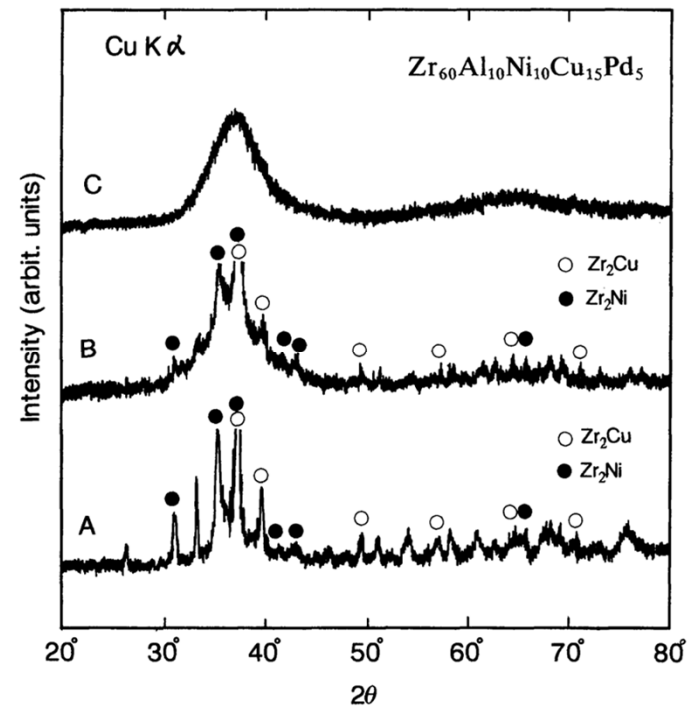


Fig. 4 Optical micrographs taken from the regions (a and b) in the transverse cross section of the cast  $Zr_{60}Al_{10}Ni_{10}Cu_{15}Pd_5$  alloy with the wedge shape of  $\theta=12.5$  degrees.





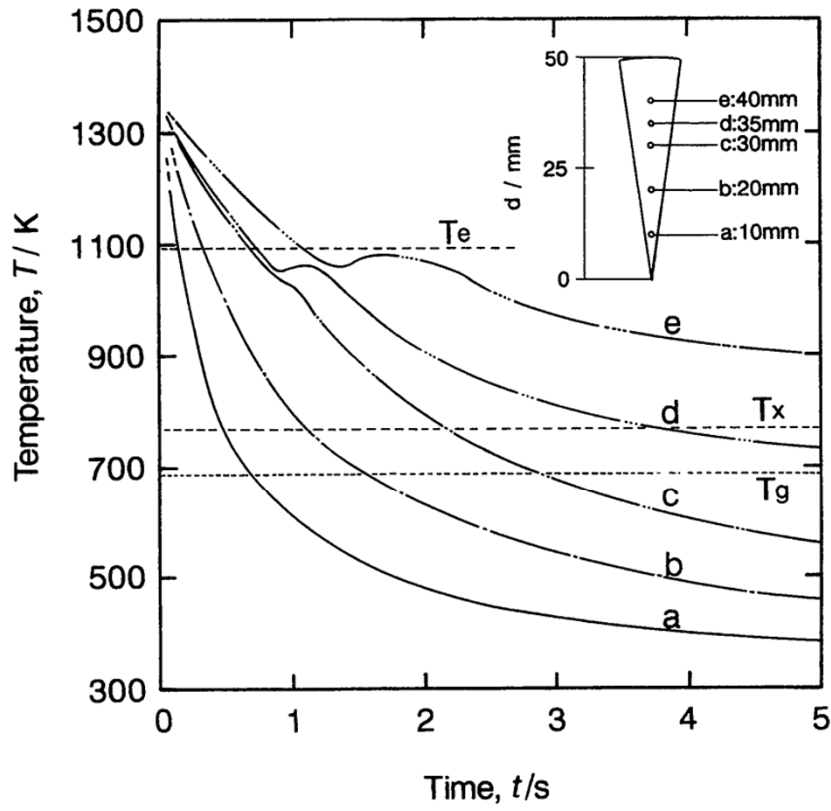


Fig. 8 Temperature-time curves at different sites (a) to (e) in the transverse cross section of the cast  $Zr_{60}Al_{10}Ni_{10}Cu_{15}Pd_5$  alloy with the wedge shape of  $\theta=12.5$  degrees.  $T_g$ ,  $T_x$  and eutectic temperature ( $T_e$ ) are also shown for reference.

**$R_c$ : 110K/s**

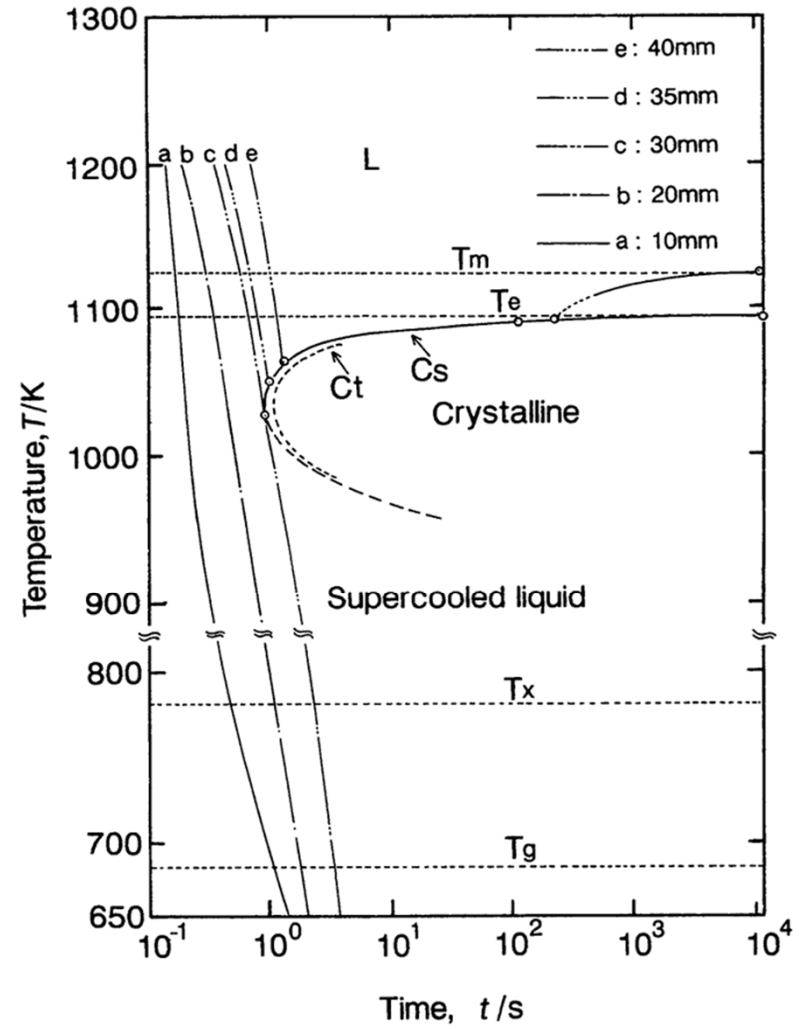
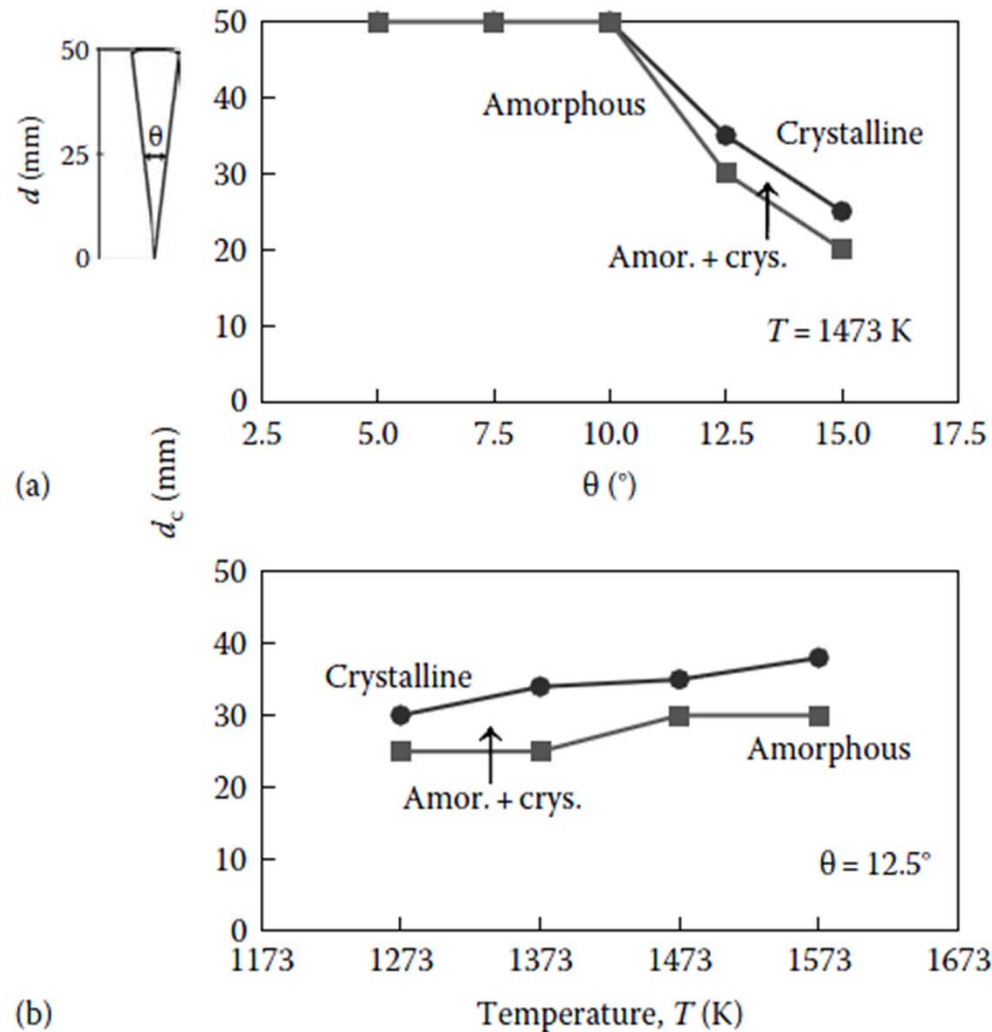


Fig. 10 Continuous-cooling-transformation (C.C.T.) curves for the transformation from supercooled liquid to crystalline phases for a  $Zr_{60}Al_{10}Ni_{10}Cu_{15}Pd_5$  alloy. The Cs and Ct represent the start and termination points of the transformation, respectively.



The height is larger for higher-pouring temperature.

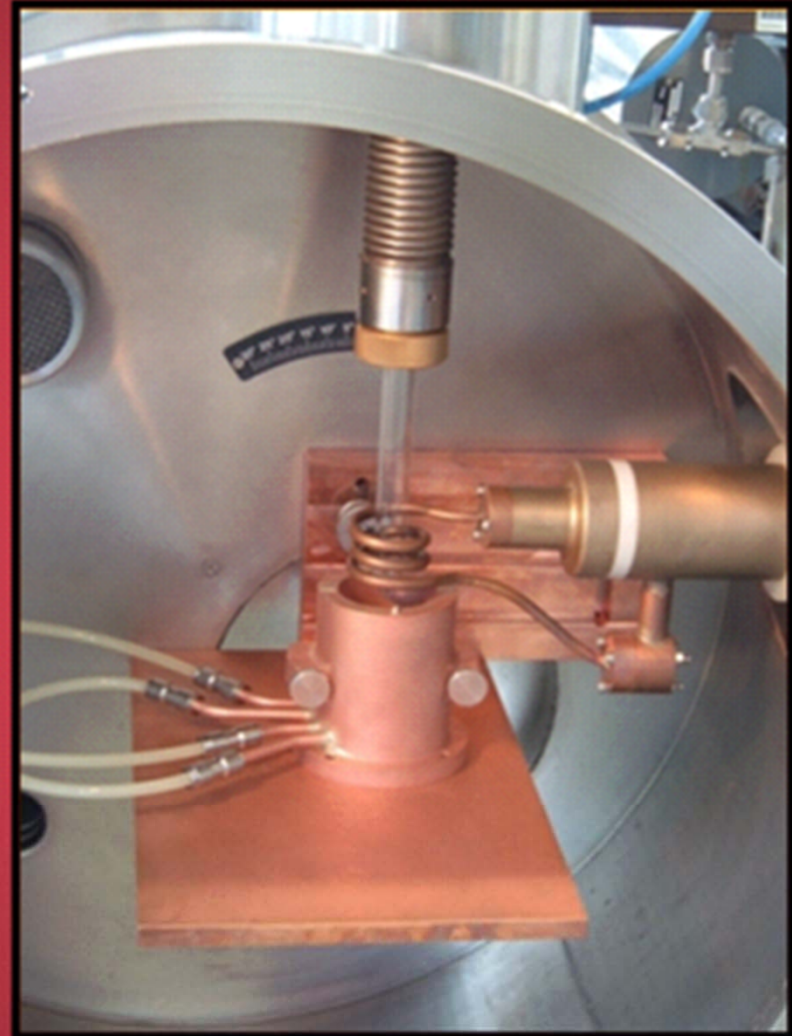
FIGURE 4.8

(a) Variation of the constitution of the alloy as a function of the height of the sample from the bottom of the wedge,  $d_c$  and the vertical angle,  $\theta$ . The figure shows the region of formation of the fully glassy phase when the  $Zr_{60}Al_{10}Ni_{10}Cu_{15}Pd_5$  alloy was ejected into the copper mold cavity at a temperature of 1473 K. (b) Variation of  $d_c$  with ejection temperature of the molten metal for the  $Zr_{60}Al_{10}Ni_{10}Cu_{15}Pd_5$  alloy cast into a wedge-shaped mold with a vertical angle  $\theta = 12.5^\circ$ . (Reprinted from Inoue, A. et al., *Mater. Trans., JIM*, 36, 1276, 1995. With permission.)

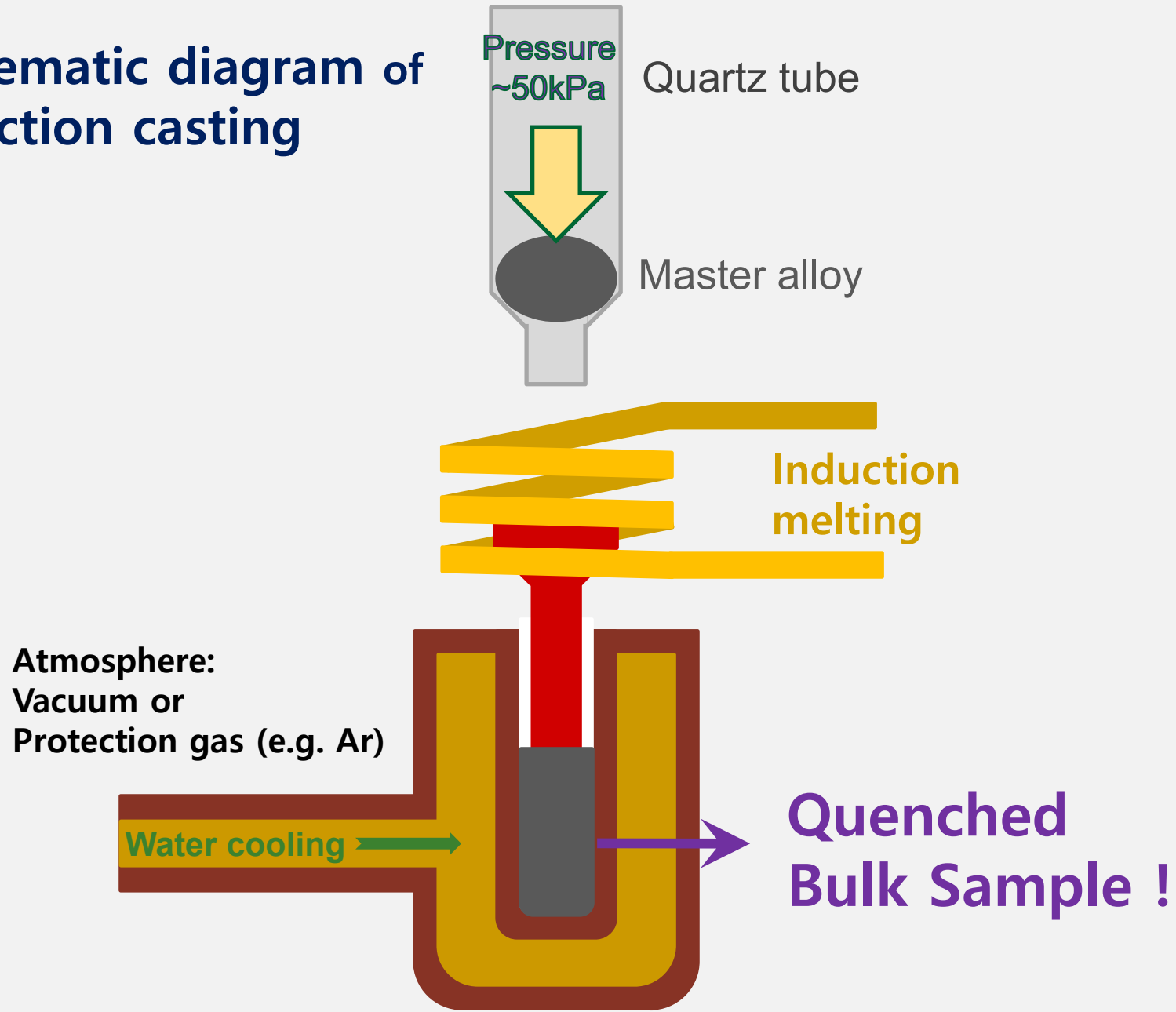
Bulk sample: rod

# Injection casting

- Simple casting method for preparing bulk samples
- Cooling medium :  
Cu mold with water cooling
- Max. cooling rate for rod sample with
  - D=5mm :  $\sim 10$  K/s
  - D=3mm :  $\sim 10^2$  K/s



# Schematic diagram of Injection casting



# Injection cast BMG samples

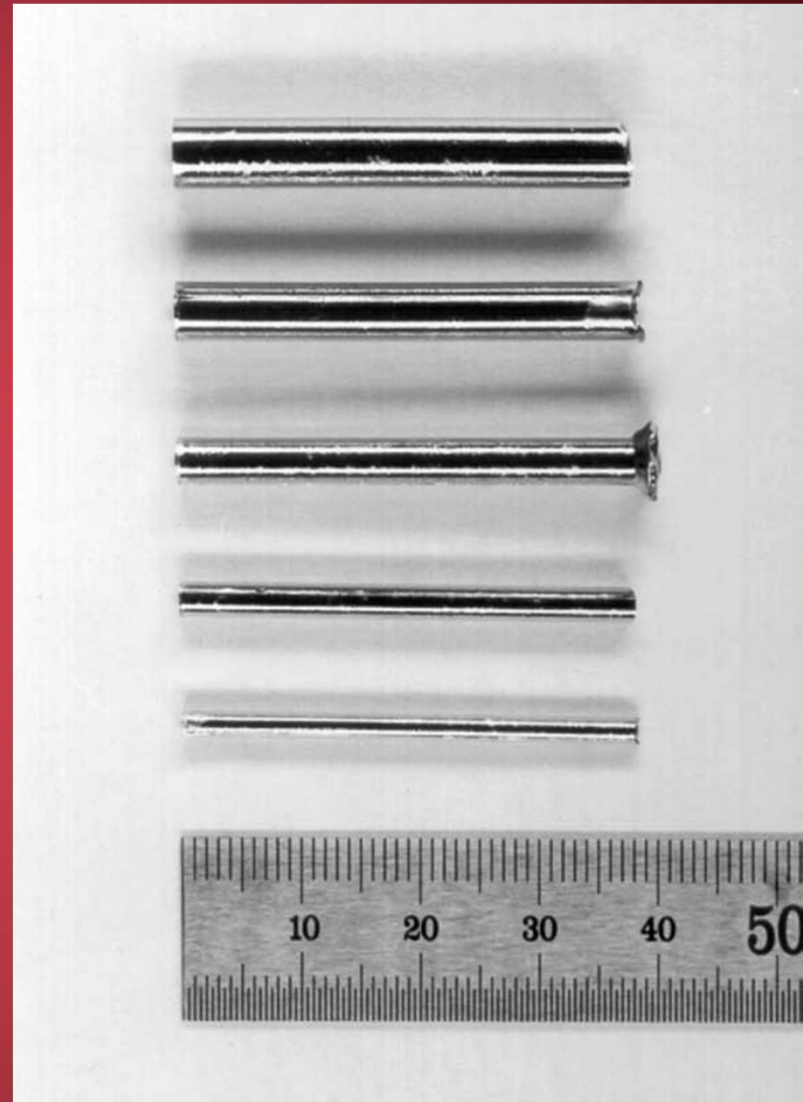
- $\text{Cu}_{47}\text{Ti}_{33}\text{Zr}_{11}\text{Ni}_6\text{Sn}_2\text{Si}_1$   
Alloy samples with diameter from 2 to 6 mm
- Cooling rate can be controlled by changing cavity diameter of mold.
- Cooling rate ( $R_c$ )

$$R_c = K(T_m - T_g)/(r^2 C)$$

$$\cong 10/r^2 \text{ (cm)}$$

K : Thermal conductivity

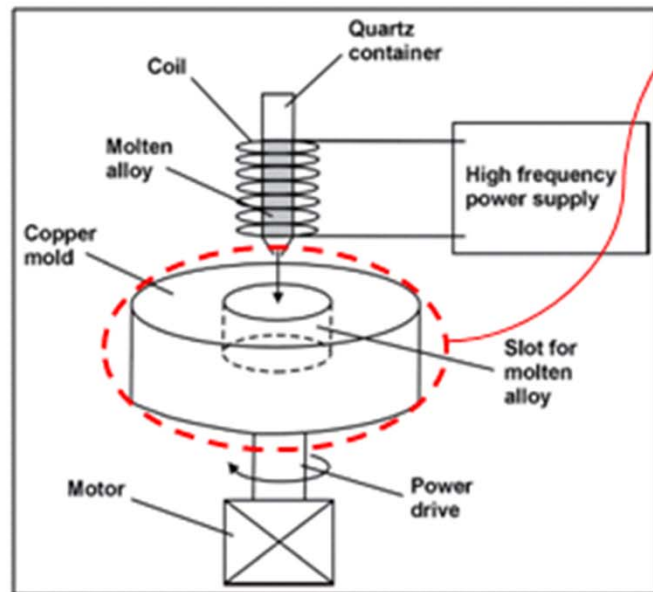
C : Specific heat capacity



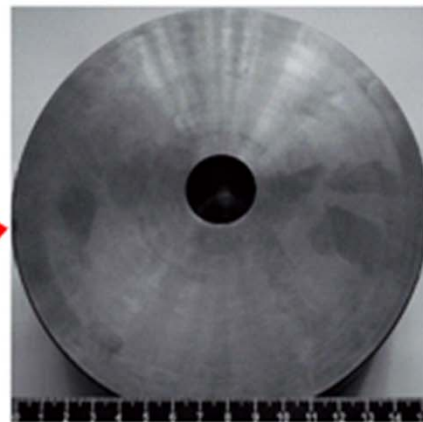
Bulk sample: tube

# Centrifugal Casting Method

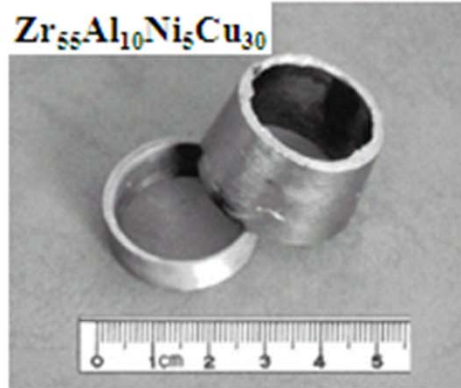
Seoul National University



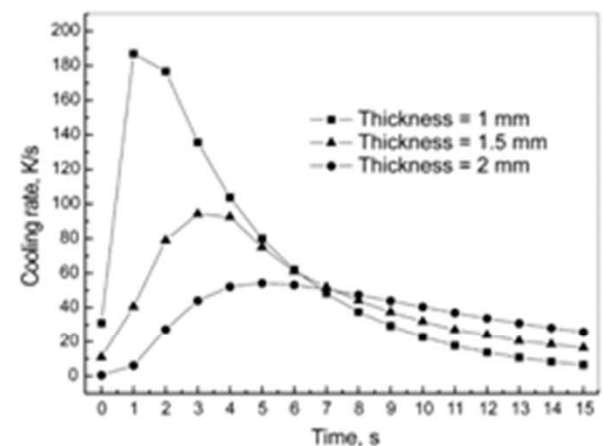
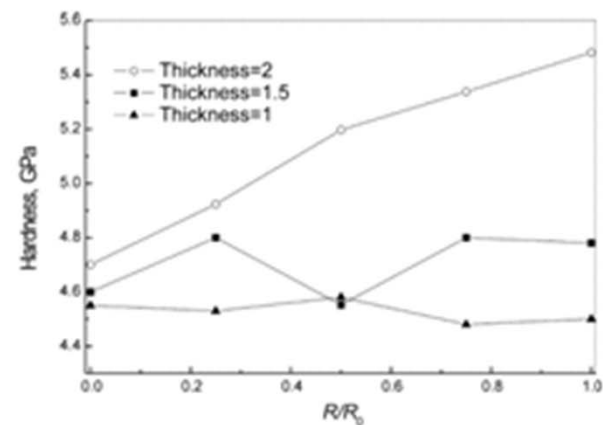
Schematic Diagram



Copper Mold



Product

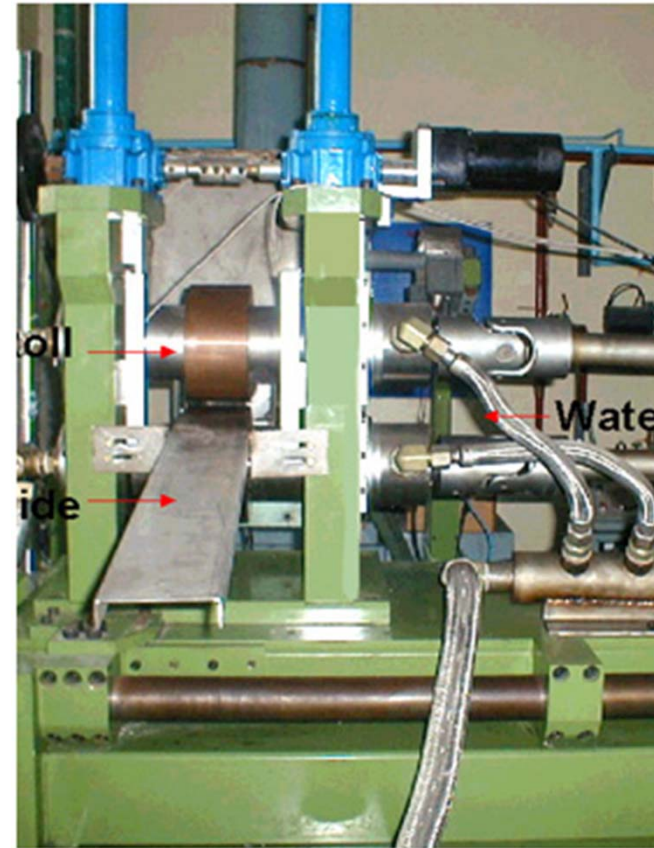
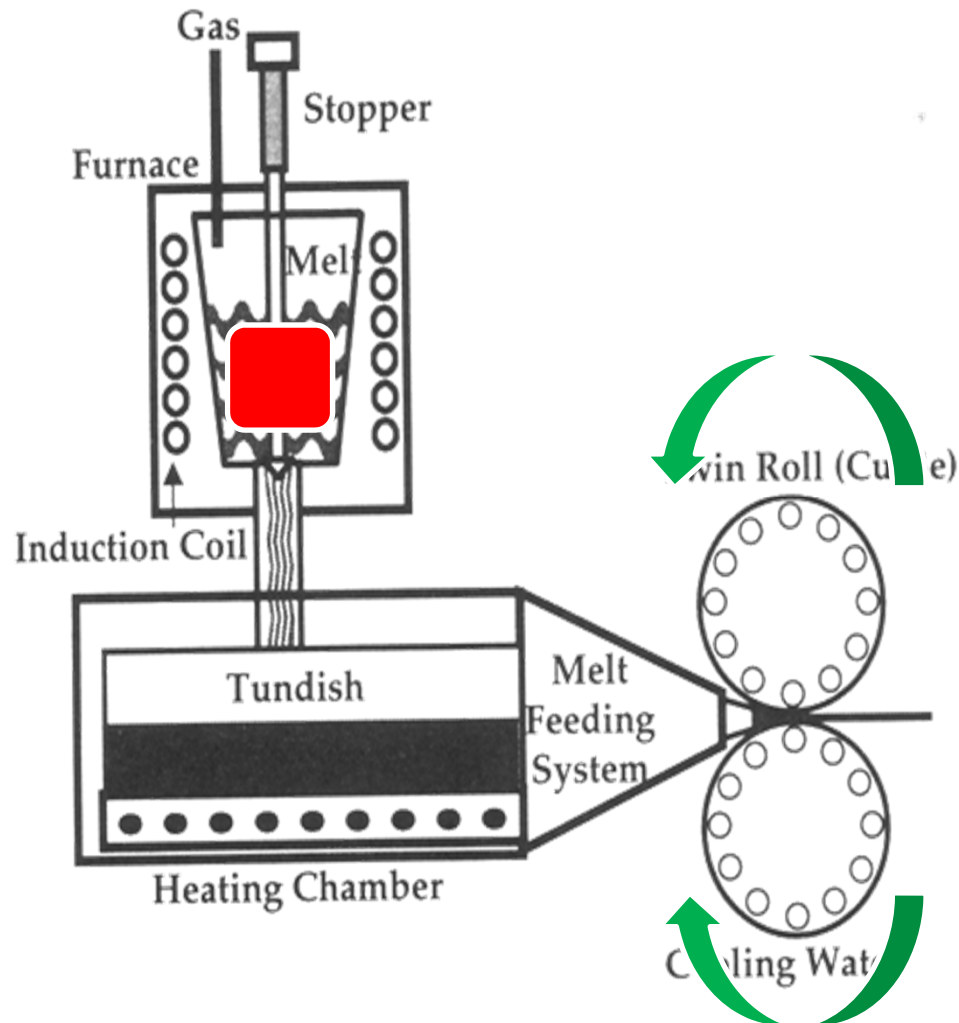


R. Nowosielski *et al.*, *J. Ach. in Mater. Man. Eng.*, Vol.20 (2007) pp.487-490  
Q. Zhang *et al.*, *Intermetallics* Vol.10 (2002) pp.1197-1201



**Bulk sample: Plate**

## Strip casting of amorphous alloys



Developed in Postech, 2004

Thickness : 1 to 4 mm

**Amorphous alloy** or  
**Amorphous + Crystalline Composites**

\* 최근 개발 내용 (RIST)

1. 2006-03-15-RIBA\_503\_소형주조-냉각  
: Fe계 비정질 판재 **twin roll strip casting**  
공정으로 제조 (gas+ moisture 급냉 공정 추가)



2. Fe-42Ni\_용탕인출공정  
: 용탕인출 공정(**melt drag / single roll strip casting**) 공정으로 invar 합금판재 제조



3. 저융점\_고속\_Melt drag (MD)  
: **MD** 공정을 이용한 벌크비정질(LM1B) 합금판재 제조





## 4.6 Bulk Metallic Glass Casting Methods

### 4.6.5 Suction-Casting Method : another popular method of synthesizing BMGs

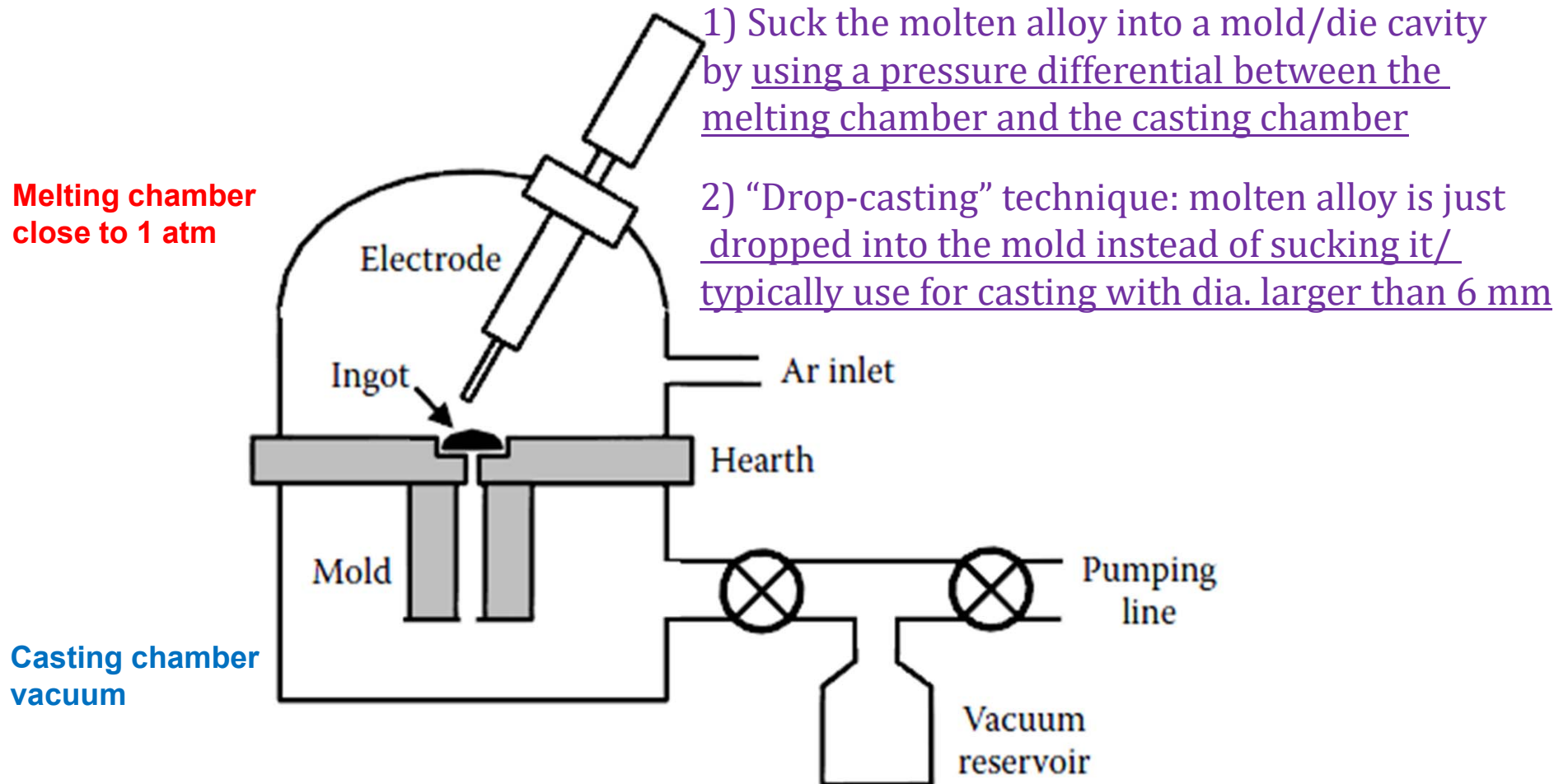
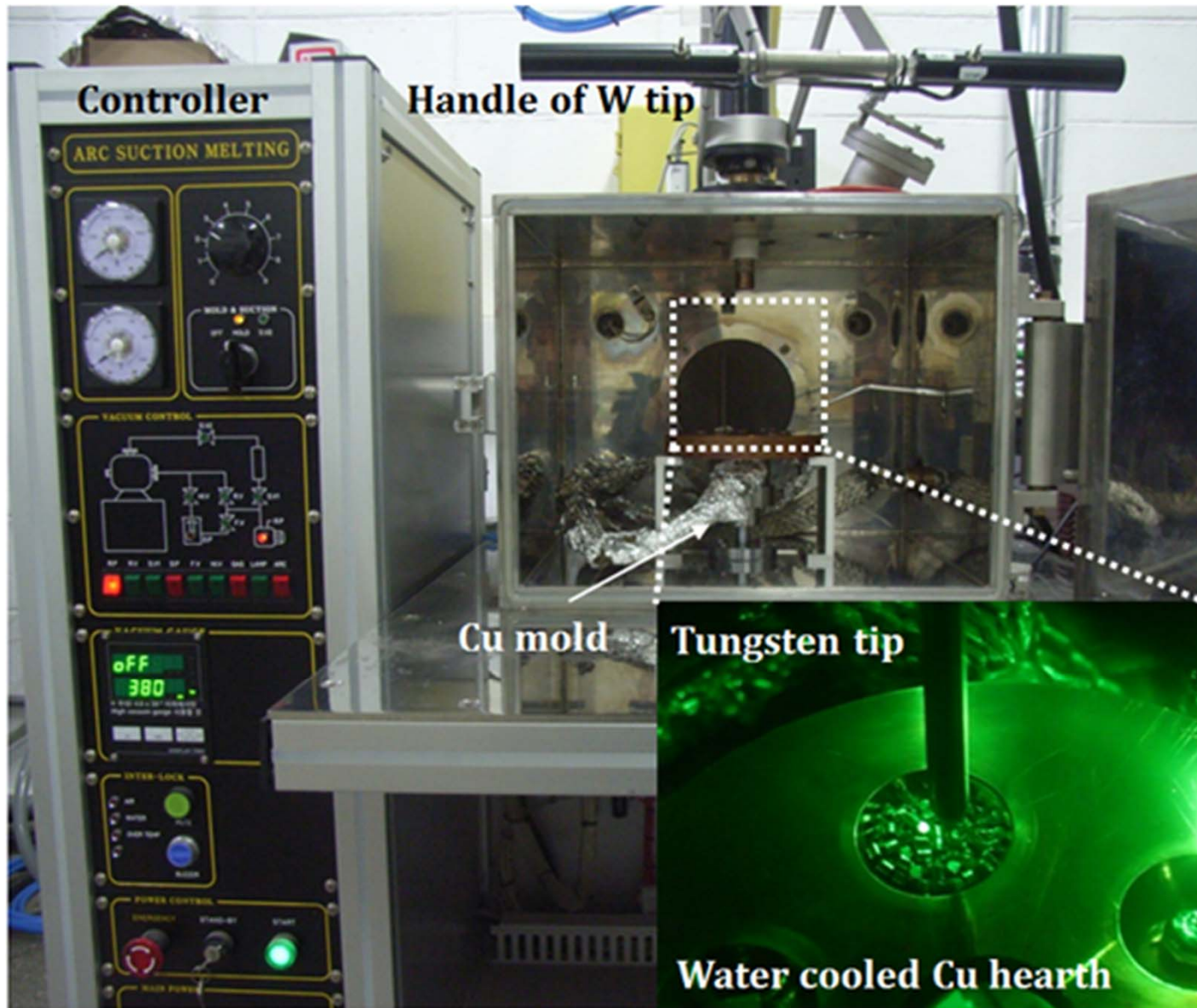


FIGURE 4.11

Schematic diagram of the arc melting/suction casting apparatus. (Reprinted from Gu, X. et al., *J. Non-Cryst. Solids*, 311, 77, 2002. With permission.)

Bulk sample: rod

## Suction Casting Method



## Suction Casting Method

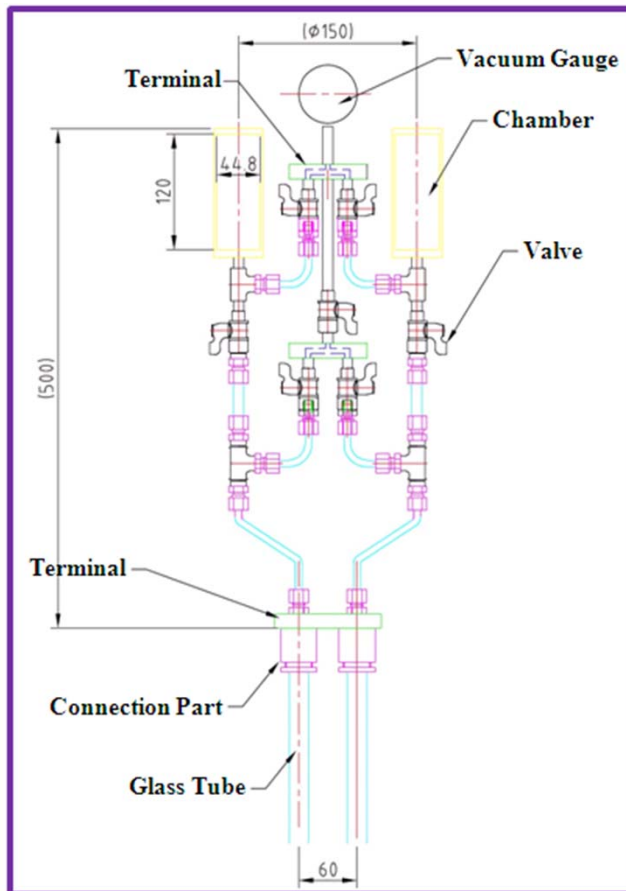


Fig. 6. Photograph of the as-cast specimens of (from left to right):  
(a) suction cast 12X1X~70 mm<sup>3</sup> plate,  
(b) drop cast 6.4X~70 mm<sup>2</sup> cylinder,  
(c) suction cast 3 mm diamX~70 mm cylinder.

A glowing green circular light in a dark environment, possibly a lens or a light source. The light is bright and circular, with a dark green stem or tube extending upwards from its center. The background is dark and slightly out of focus, showing some faint circular patterns.

Created with FlipMac WMV Demo  
[www.flipmac.com](http://www.flipmac.com)

## 4.6 Bulk Metallic Glass Casting Methods

### 4.6.7 Arc-Melting Method

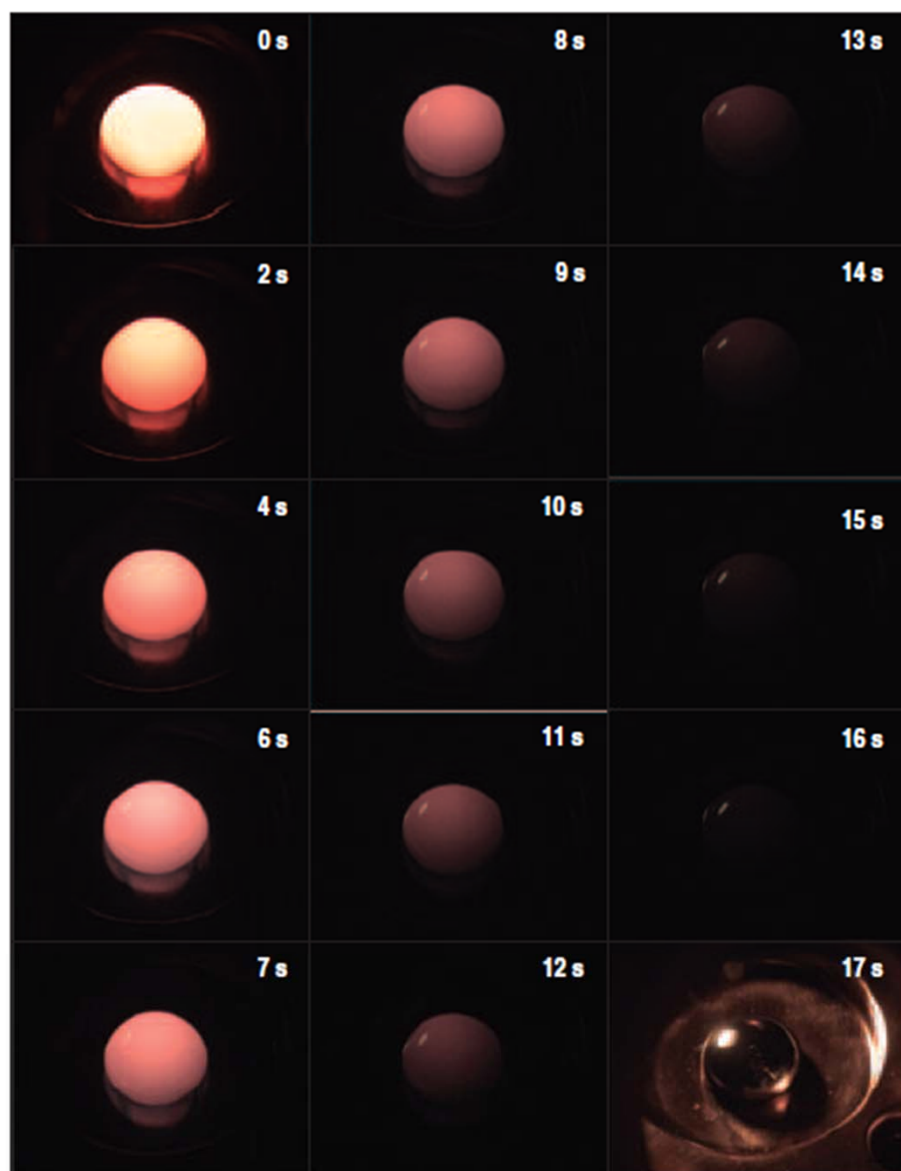
**Who can explain the clear difference between two movies?**



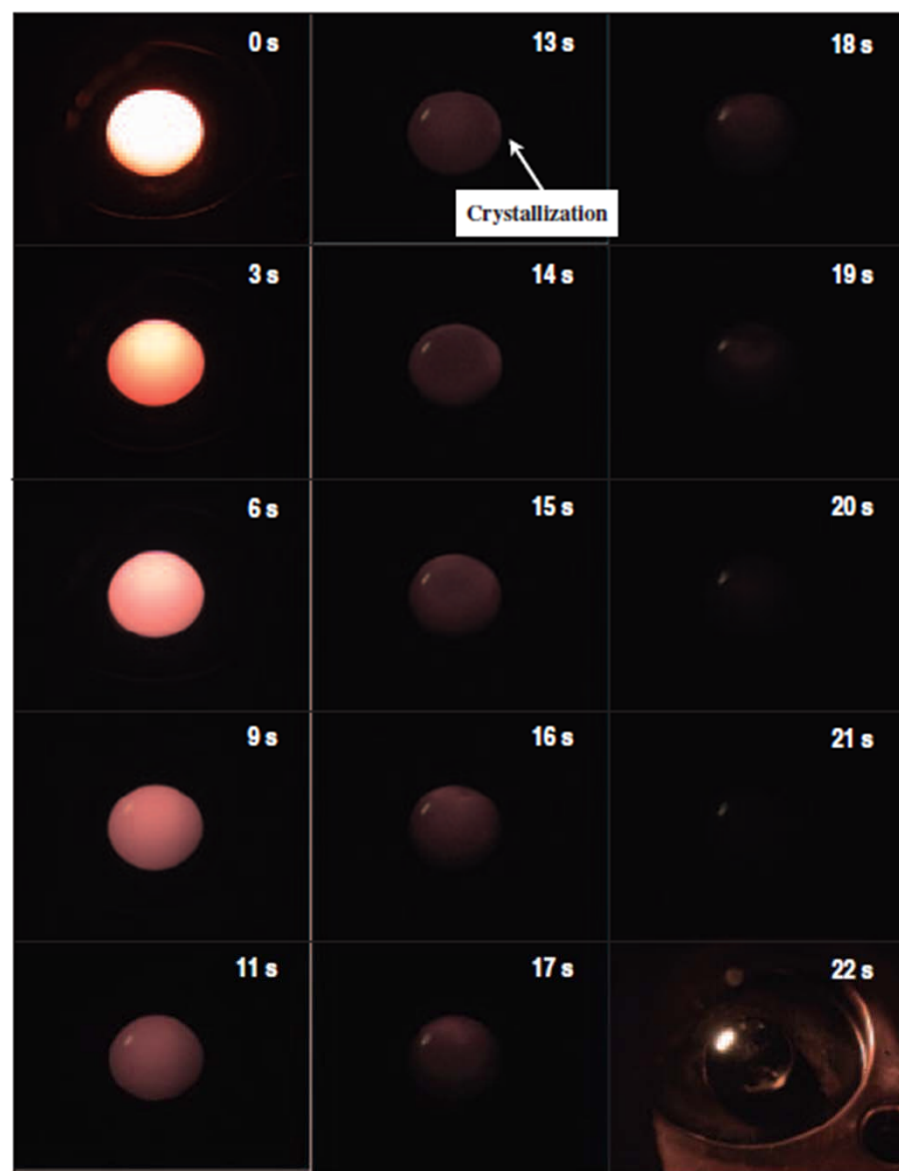
**ZrCuAl alloy with purified Zr**



**ZrCuAl alloy with non-purified Zr**



ZrCuAl alloy with purified Zr



ZrCuAl alloy with non-purified Zr

## Glassy Solidification Criterion of $Zr_{50}Cu_{40}Al_{10}$ Alloy

Yoshihiko Yokoyama<sup>1</sup>, Hasse Fredriksson<sup>2</sup>, Hideyuki Yasuda<sup>3</sup>,  
Masahiko Nishijima<sup>1</sup> and Akihisa Inoue<sup>1</sup>

<sup>1</sup>Institute for Materials Research, Tohoku University, Sendai 980-8577, Japan

<sup>2</sup>Department of Materials Processing Casting of Metals, SE-100 44 Stockholm, Addr. Brinellvagen 23, Sweden

<sup>3</sup>Department of Adaptive Machine Systems, Osaka University, Osaka 565-0871, Japan

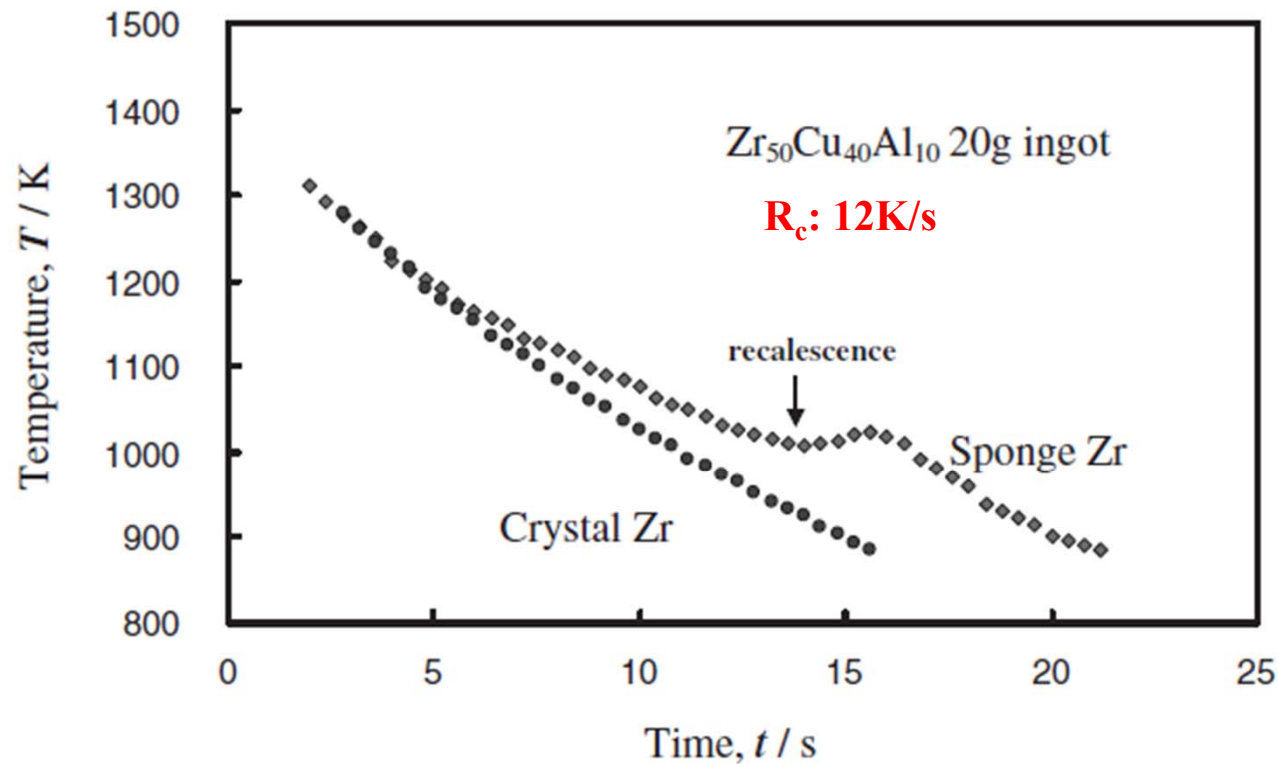
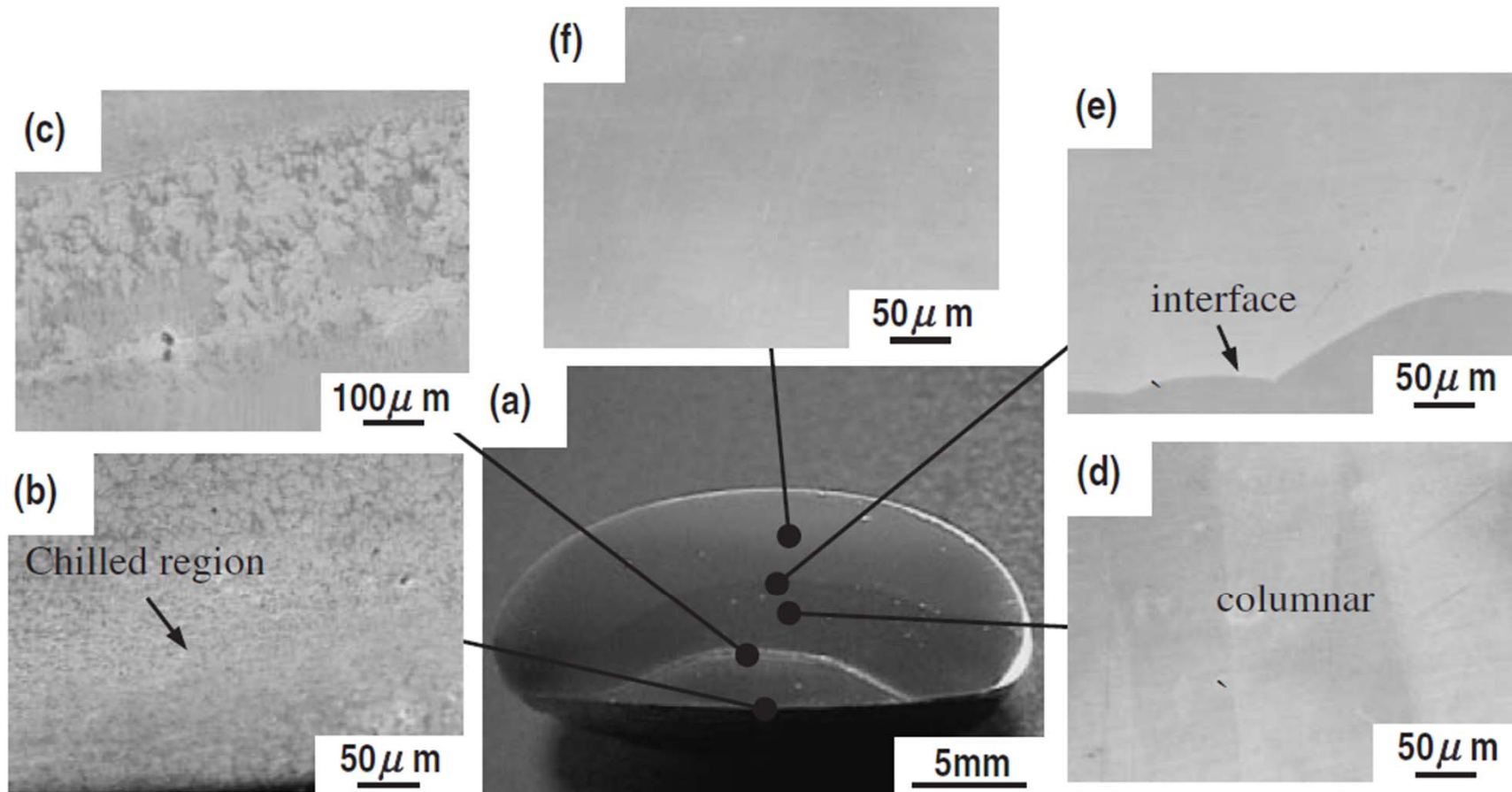


Fig. 6 Cooling curves of arc-melted  $Zr_{50}Cu_{40}Al_{10}$  ingots with crystal Zr and sponge Zr.

# Drawback in Arc Melting:

the ease of heterogeneous nucleation due to incomplete melting of the alloy at the bottom side that is in contact with the copper hearth



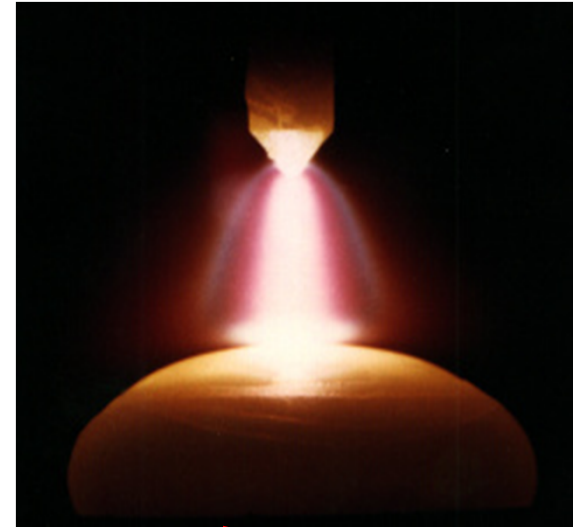
OM images of an arc-melted 20-g  $Zr_{50}Cu_{40}Al_{10}$  ingot with crystal Zr (a) and magnified partial images (b~e).



# Drawback in Arc Melting

## Cold Spot (position)

Interface between molten alloy and Cu hearth

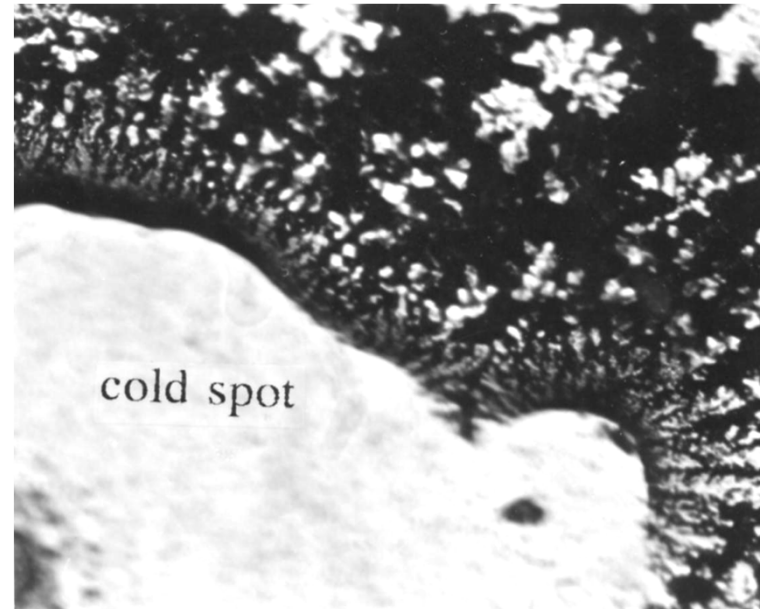


## Cold Spot (act)

Spring of crystalline particles

## Cold Spot

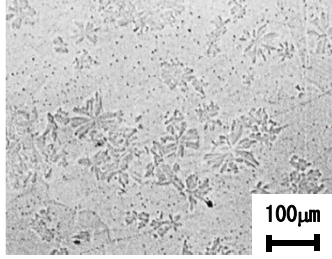
should be controlled !



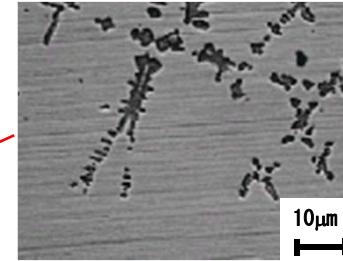
# Crystalline Particles observed in cast Zr-Cu-Al BMGs

FCC (unknown)  
Mater. Trans.,  
Vol.45, No.6 (2004)  
1819-1823

## 2. Oxygen absorption?

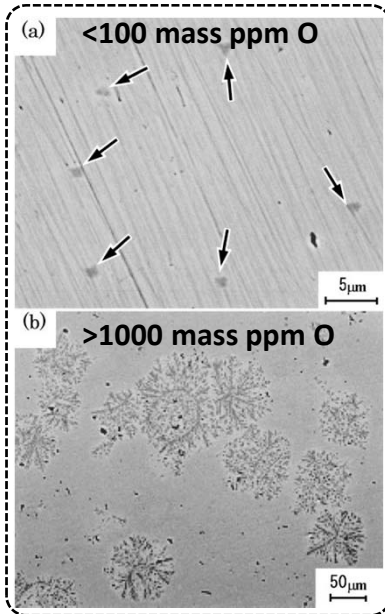


## 1. Insufficient alloying for homogenizing?

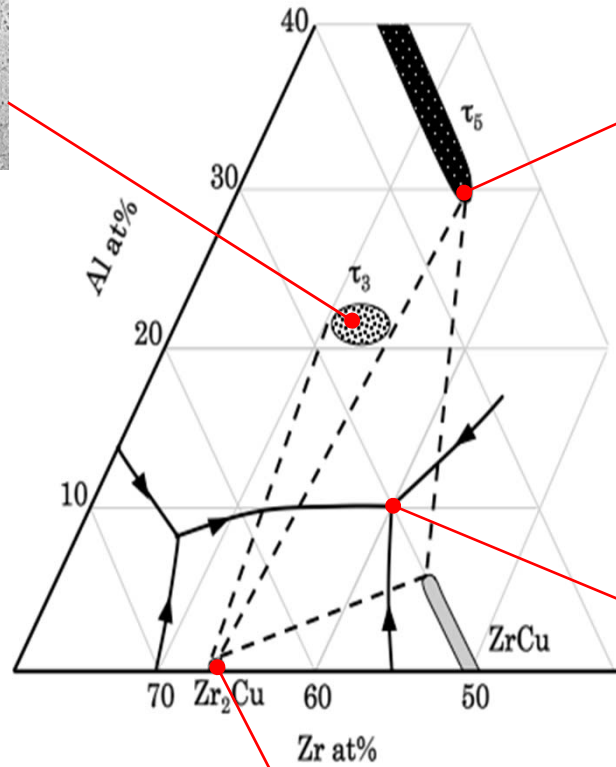
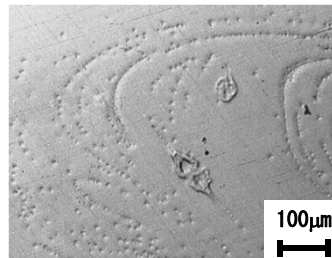


Hexagonal Laves ( $\text{Al}_2\text{Zr}$ )

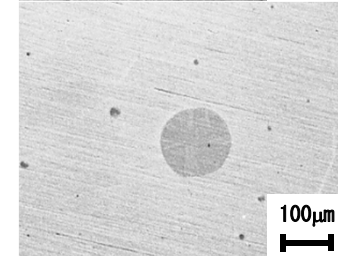
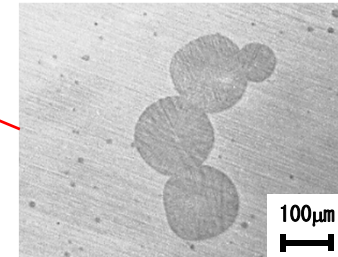
Oxygen enhance the growth of  $\tau_3$



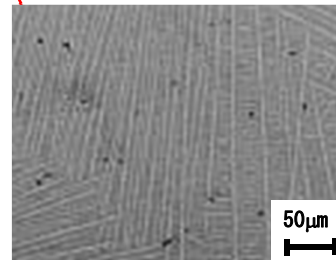
Cold shuts with  $\tau_3$  dendrites



## 3. Spherulite (Impurities?)



Composite structures



Tetragonal ( $\text{Zr}_2\text{Cu}$ )

## 4.6 Bulk Metallic Glass Casting

**4.6.4 Cap-Cast Technique:** bringing a metallic cap into contact with the molten metal, and applied a small pressure of about 1 kN → high CR

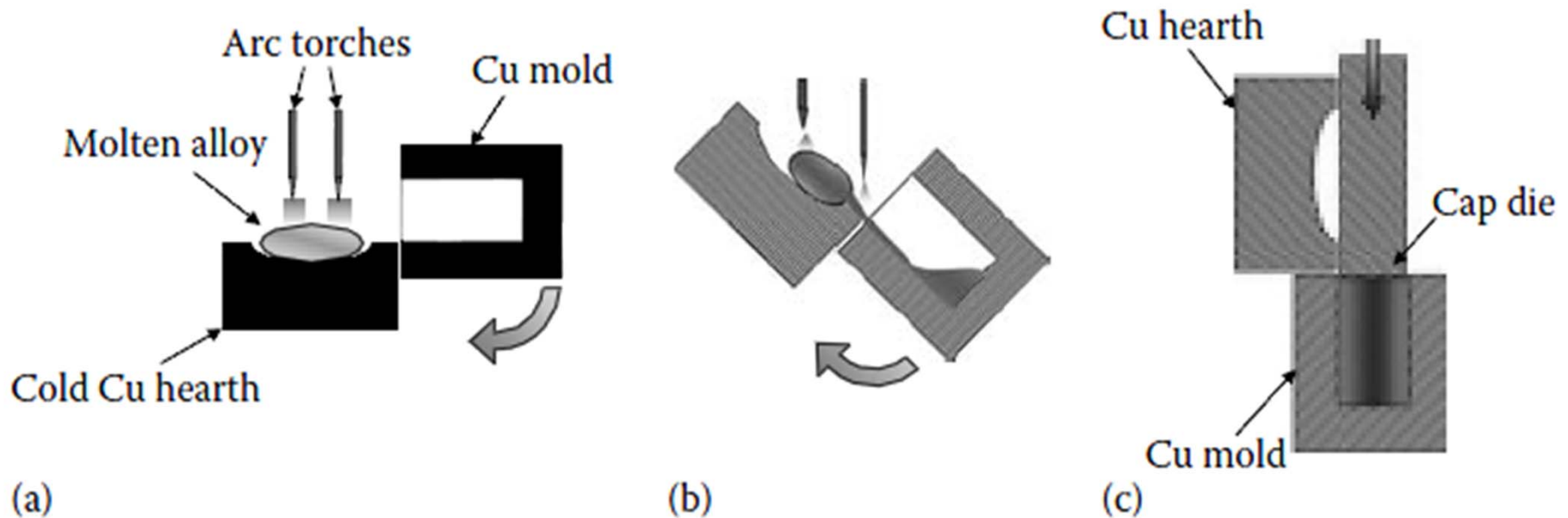


FIGURE 4.9

Schematic diagrams comparing the (a) arc melting, (b) tilt casting, and (c) cap-cast techniques used to produce bulk metallic glassy alloys.

$Zr_{55}Cu_{30}Ni_5Al_{10}$   $D_{max} = 16$  mm using conventional metallic mold casting  
→  $D_{max} = 30$  mm using cap-casting technique : GFA ↑

## New Tilt-Cast Machine for Centimeter Sized BMG



$\Phi 30\text{mm}$   $\text{Zr}_{55}\text{Cu}_{30}\text{Ni}_5\text{Al}_{10}$  BMG rod

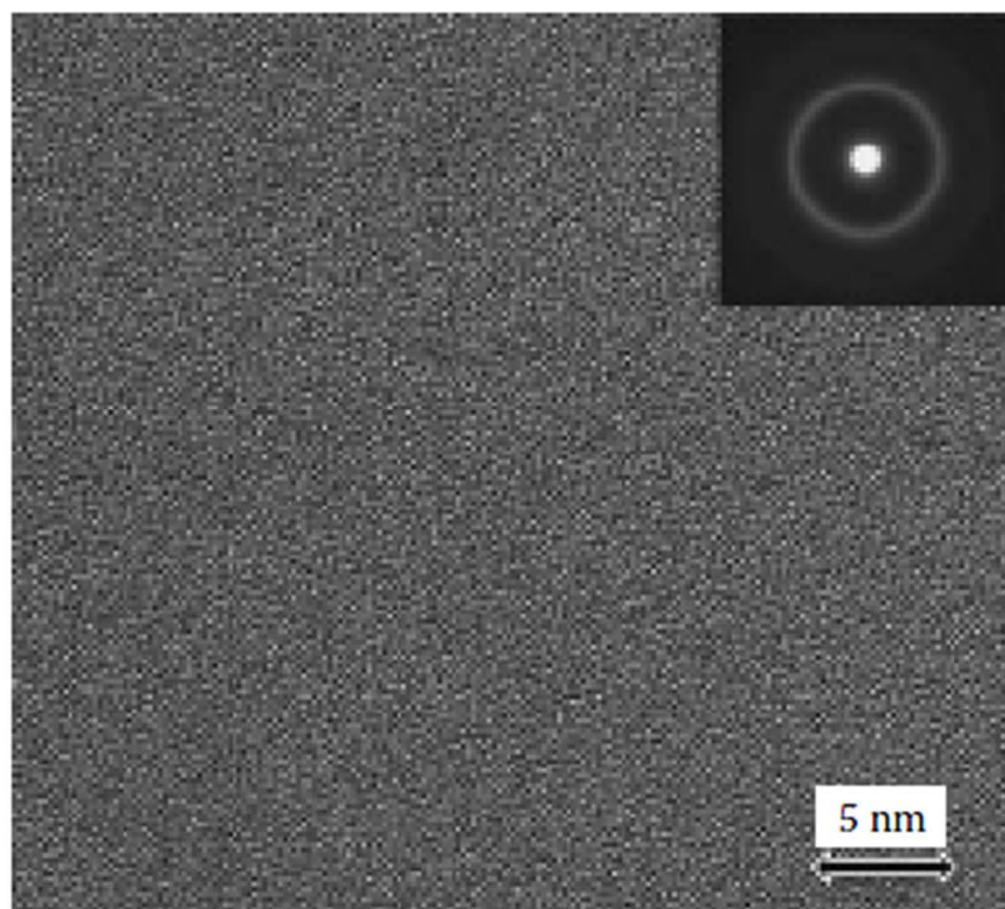
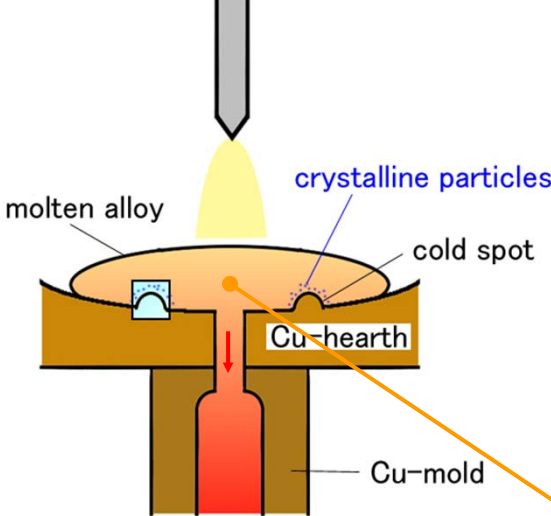


**FIGURE 4.10**

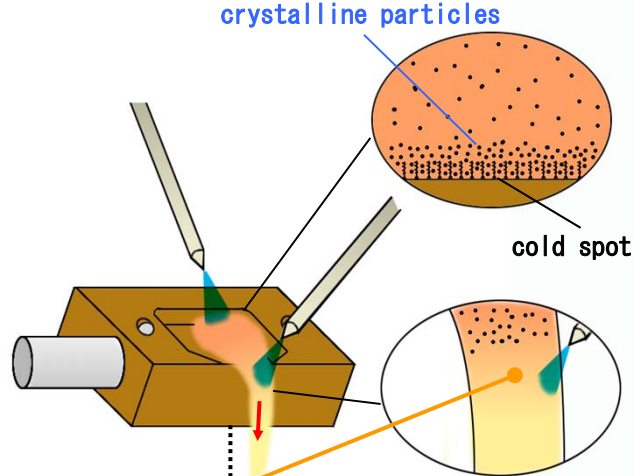
High-resolution transmission electron micrographs of cap-cast  $Zr_{55}Cu_{30}Ni_5Al_{10}$  glassy alloy of 30 mm diameter. The micrograph was recorded from the center of the sample at the site 10 mm from the bottom of the casting. No fringe marks are seen even on a nanometer scale, suggesting that the whole sample was fully glassy.

# How to control the Cold Spot in Arc Melting/Casting1

(a) Cold Cu Nozzle



(b) Ladle Hearth

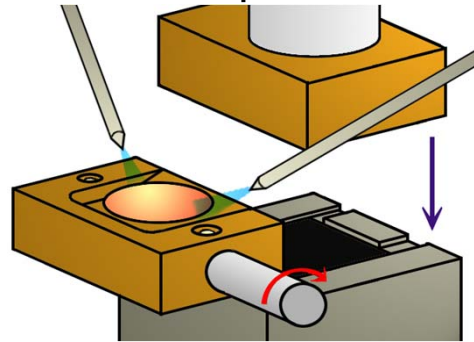
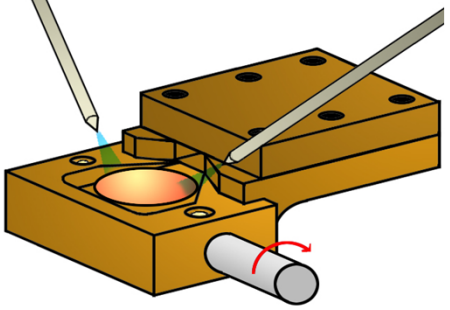


complete melting

applied for

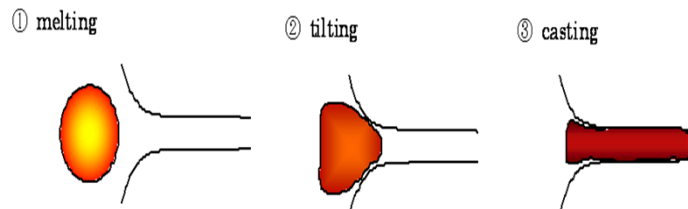
tilt casting

squeeze casting

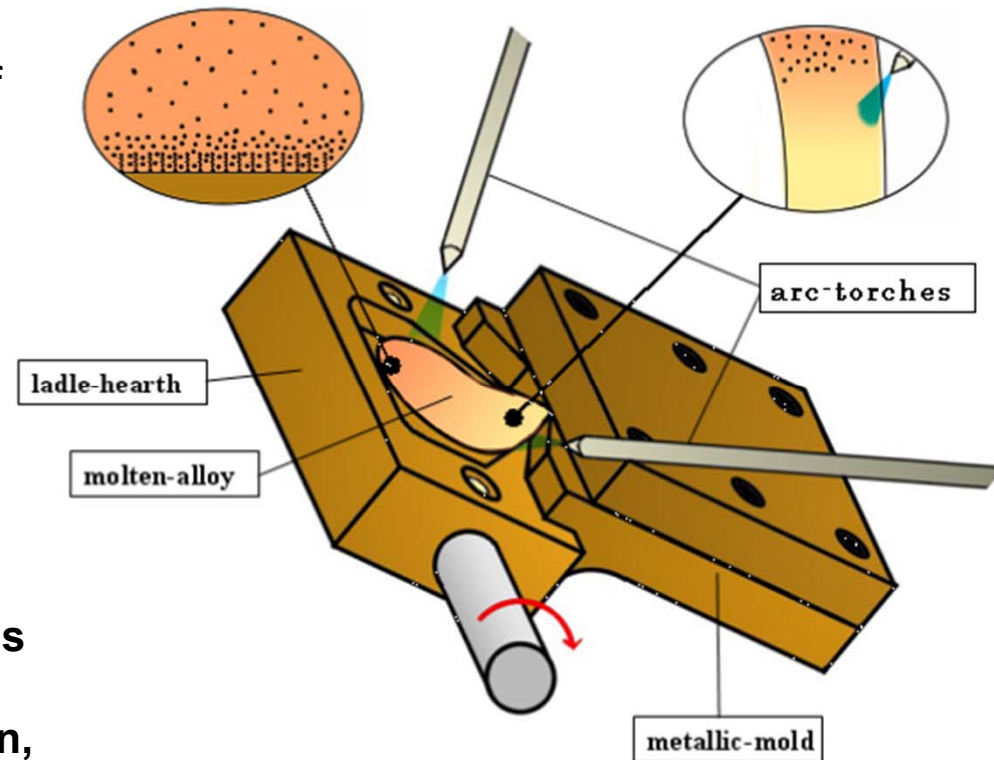


# Cold shut / An Advantage of Arc Tilt Casting

**Tilt Casting** has an advantage to restrict the formation of **cold shut**, because of much smaller change of surface area of molten alloy during casting than other casting techniques..



**Cold shut**, which probably acts as crack initiation site and contributes crack propagation, is regarded as a discontinuous plate defect formed by two streams of liquid meeting.



JPN Patent No. 4164851

# Fabrication of amorphous materials-tilt casting

- reduce porosity and inclusions by limiting turbulence
- If the system is rotated slow enough to not induce turbulence, the front of the metal stream begins to solidify.
- If the system is rotated faster then it induces turbulence, which defeats the purpose.





# Automatic Production Process of BMGs

- Human Error → **Automatic Production Process**
- Depending on Technical Skill ↑
- Homogeneity → small quantity, melting: long time, flipping: many times

**1. Automatic Weighing Machine [Patent preparation]**



**2. Automatic Arc-Melt Furnace [2009-118159]**

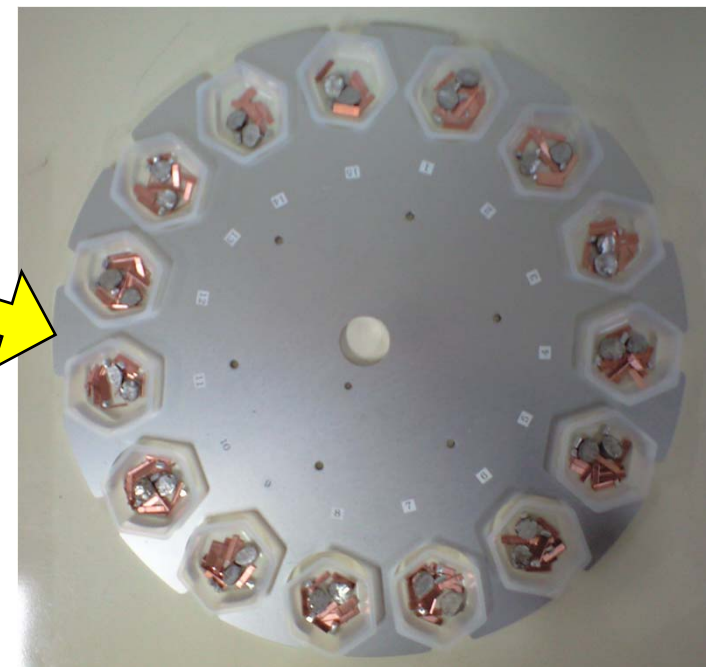
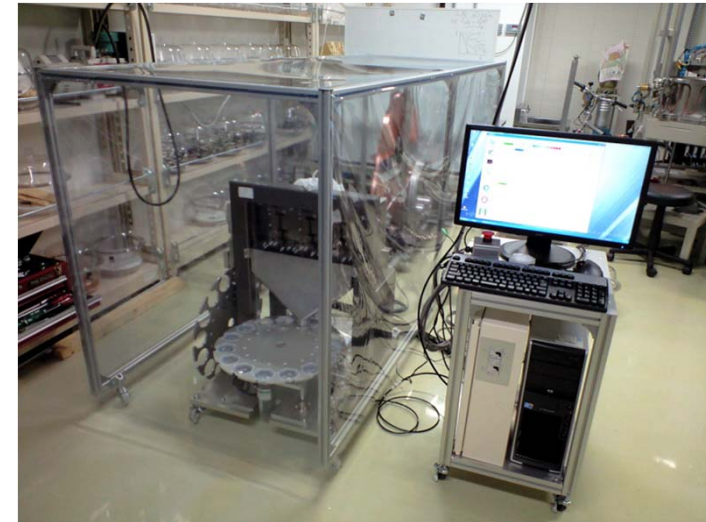
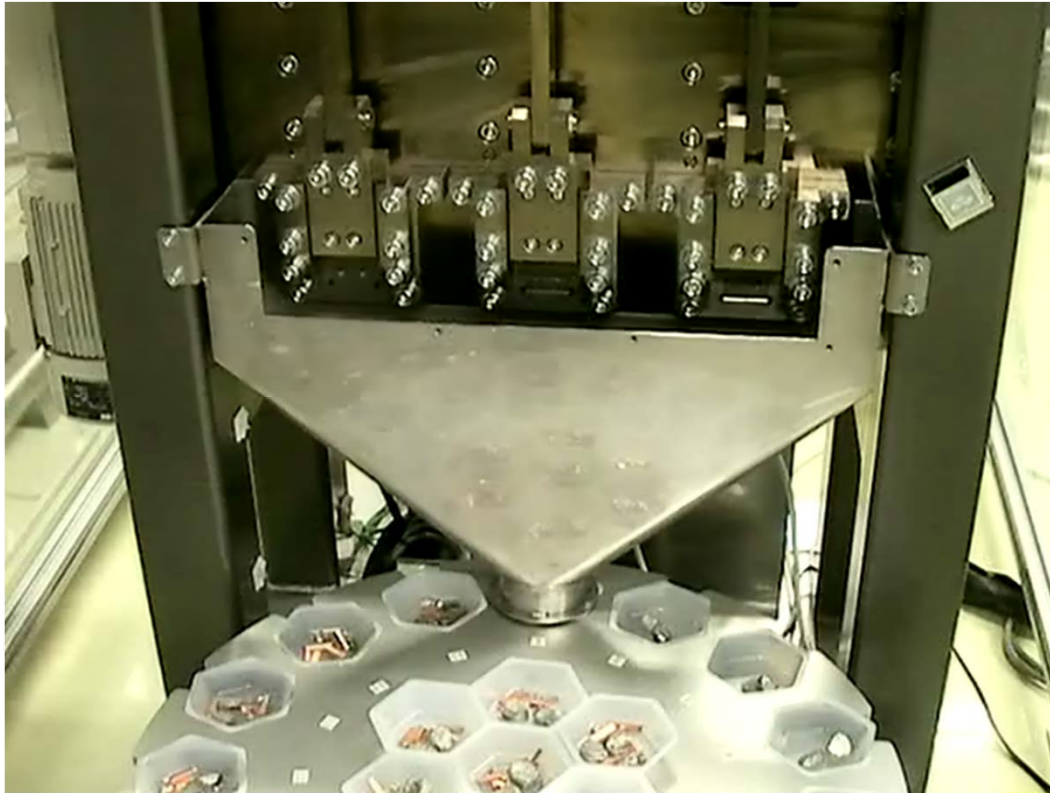


**3. Automatic Casting Machine [2008-283129]**



**Almost 30 master alloy ingots (1 kg) can be produced within 7 hours.... ~100 alloys/day**

# Automatic Weighing Machine for BMG Master Alloys



*Tohoku Techno Arch Co. Ltd*

<http://www.t-technoarch.co.jp/en/index.html>

~100,000 US \$

# Automatic Arc-Melt Furnace for BMG Master Alloys



Reference ; <http://www.diavac.co.jp/>

## Automatic Casting Machine for BMGs



*Tohoku Techno Arch Co. Ltd* <http://www.t-technoarch.co.jp/en/index.html>

# Squeeze Casting Technique



[Patent submitted]

# Automatic Casting Machine for BMGs



# Enveloped Cast Technique for BMG Parts (hip joint)

For biomedical use



Stainless Steel (core)

Ball head was covered by BMG with enveloped casting (thickness 3 mm)



# 4.6 Bulk Metallic Glass Casting Methods

## 4.6.8 Unidirectional Zone Melting Method

Materials Transactions, JIM, Vol. 35, No. 12 (1994), pp. 923 to 926

RAPID PUBLICATION

### Preparation of Bulky Zr-Based Amorphous Alloys by a Zone Melting Method

Akihisa Inoue, Yoshihiko Yokoyama, Yoshiyuki Shinohara† and Tsuyoshi Masumoto

Institute for Materials Research, Tohoku University, Katahira 2-1-1, Sendai 980-77, Japan

A bulk amorphous  $Zr_{60}Al_{10}Ni_{10}Cu_{15}Pd_5$  alloy was prepared by the zone melting method using an arc-type heat source. The bulk amorphous alloy prepared on the copper hearth has a rectangular parallelepiped shape with a thickness of 10 mm, a width of 12 mm and a length of 170 mm. A majority of the region except the bottom and side edge regions contacted with copper hearth consists of an amorphous phase. The cooling rate achieved by the zone melting method is high enough to cause an amorphous phase in the Zr-based alloy where heterogeneous nucleation is suppressed. The amorphous phase subjected to continuous heating exhibits a distinct glass transition, followed by a wide supercooled liquid region and then an exothermic peak due to crystallization. The success of producing the bulk amorphous alloys by the zone melting method implies the possibility of the continuous production of the bulk amorphous alloys and seems to accelerate the subsequent progress of amorphous alloys.

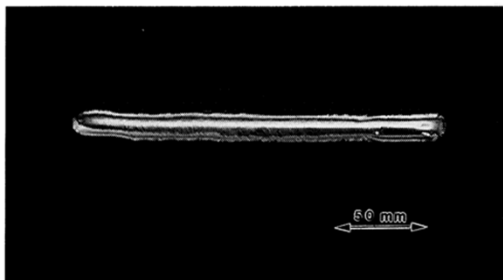


Fig. 2 Photograph revealing the outer surface appearance of a bulky  $Zr_{60}Al_{10}Ni_{10}Cu_{15}Pd_5$  alloy ingot prepared by the zone melting method.

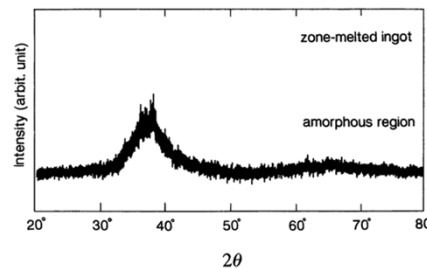


Fig. 3 X-ray diffraction pattern taken from the central region of a bulky  $Zr_{60}Al_{10}Ni_{10}Cu_{15}Pd_5$  alloy ingot in a rectangular parallelepiped shape with a thickness of 10 mm, a width of 12 mm and a length of 170 mm.

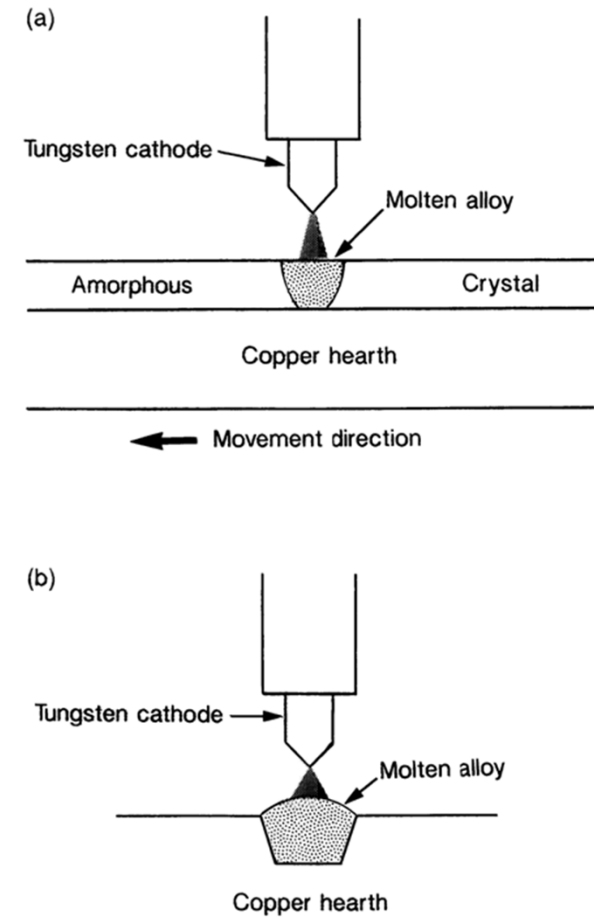
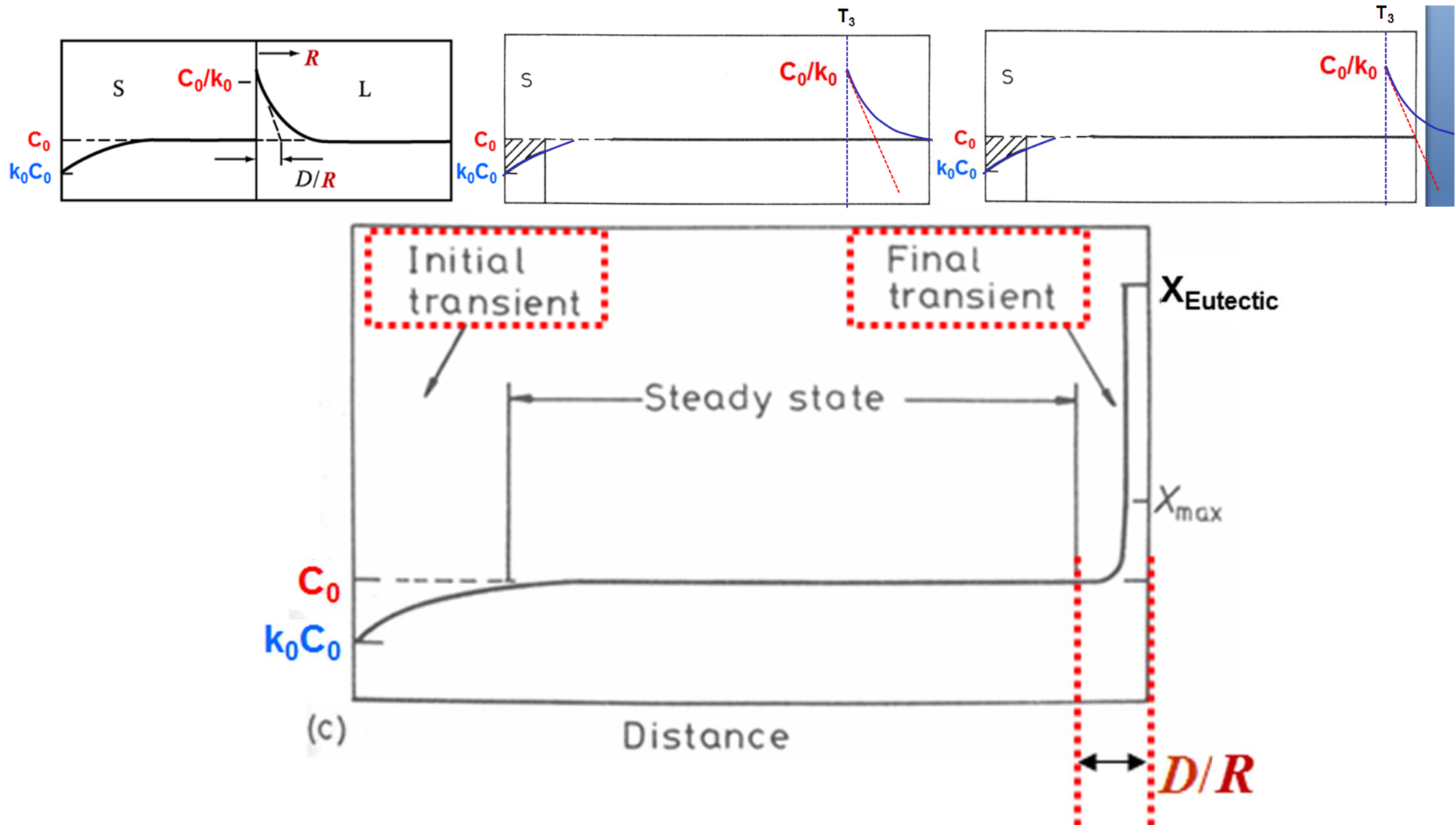


Fig. 1 Schematic illustration of the zone melting equipment using an arc electrode as a heat source which was used for the preparation of a bulk amorphous alloy ingot. (a) front view, (b) lateral view.

# “Alloy solidification” - Solidification of single-phase alloys

\* No Diffusion on Solid, Diffusional Mixing in the Liquid



When the solid/liquid interface is within  $\sim D/R$  of the end of the bar the bow-wave of solute is compressed into a very small volume and the interface composition rises rapidly leading to a final transient and eutectic formation.

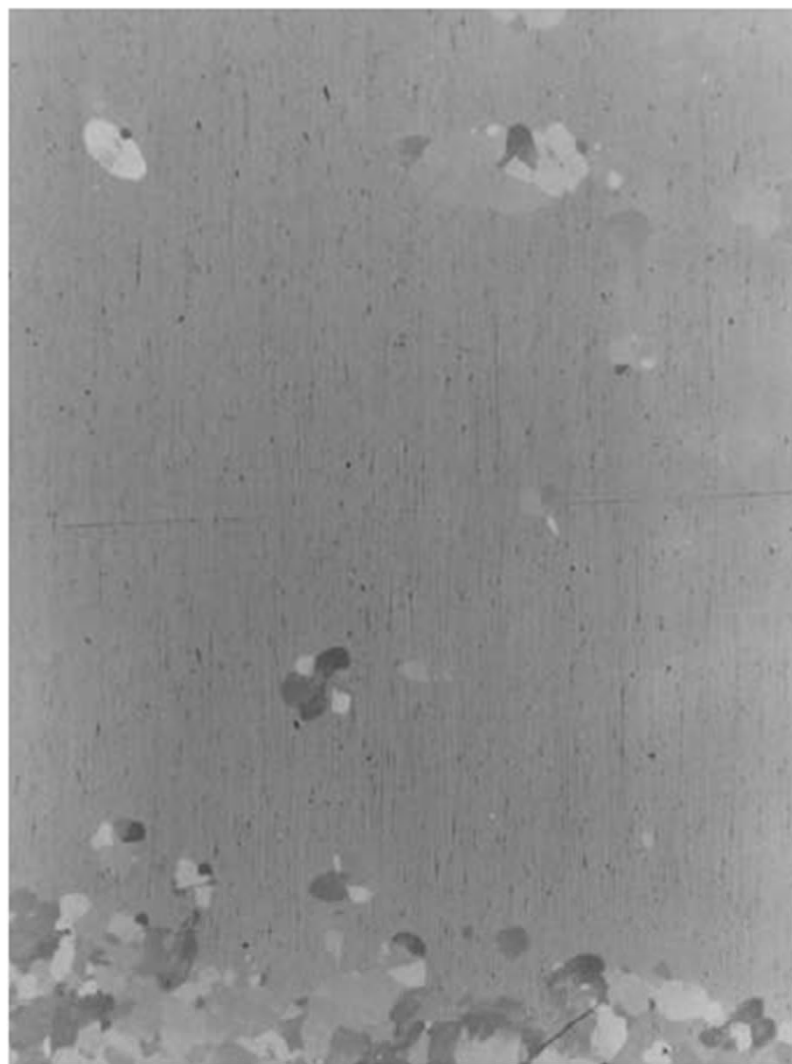


**FIGURE 4.13**

Optical micrograph of the unidirectionally zone-melted  $\text{Zr}_{60}\text{Al}_{10}\text{Ni}_{10}\text{Cu}_{15}\text{Pd}_5$  alloy ingot showing the presence of some crystals in a glassy matrix. One can notice a large volume fraction of larger (about  $200\mu\text{m}$  in size) crystals in the region close to the bottom of the ingot that is about 2 mm away from the copper hearth.

RAPID PUBLICATION

# Solidification Condition of Bulk Glassy $Zr_{60}Al_{10}Ni_{10}Cu_{15}Pd_5$ Alloy by Unidirectional Arc Melting

Yoshihiko Yokoyama and Akihisa Inoue

Institute for Materials Research, Tohoku University, Sendai 980-77, Japan

The relation between the formation of a glassy phase and the solidification parameters of moving velocity of liquid/solid interface ( $V$ ), temperature gradient ( $G$ ) and cooling rate ( $R$ ) was examined for a  $Zr_{60}Al_{10}Ni_{10}Cu_{15}Pd_5$  alloy, with the aim of clarifying a solidification condition for formation of a bulk glassy alloy by a unidirectional arc-melting method. The glassy phase was obtained in the condition of  $V > 4$  mm/s,  $G > 4$  K/mm and  $R > 40$  K/s. The decrease in  $G$  causes the formation of equiaxed dendrites, oriented dendrites and cell structure. The supercooling for the present alloy was measured to be as large as 385 K at a low cooling rate of 40 K/s. The large supercooling ability is presumably due to the formation of a highly dense random packed structure where the nucleation of a crystalline phase and the atomic rearrangement for growth reaction are difficult. The glass formation of the present multicomponent alloy in the unidirectional arc melting method seems to be dominated by the ease of the supercooling ability rather than the achievement of high cooling rate.

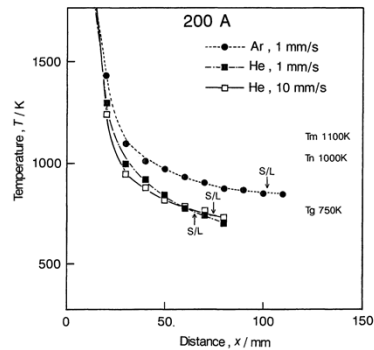


Fig. 2 Change in the temperature of the unidirectionally arc-melted  $Zr_{60}Al_{10}Ni_{10}Cu_{15}Pd_5$  ingots as a function of distance from the center of arc electrode in the case of an arc current of 200 A.

Table 1 Various solidification parameters which were experimentally measured for the unidirectionally arc-melted  $Zr_{60}Al_{10}Ni_{10}Cu_{15}Pd_5$  ingots.

A (A)	V (mm/s), (gas)	$\Delta X$ (mm)	$\Delta T$ (K)	$G_{S/L}$ (K/mm)	$G_{Noise}$ (K/mm)	$R_{S/L}$ (K/s)	$R_{Noise}$ (K/s)
200	1, Ar	102	245	0.1	33	0.1	33
	1, He	65	335	3.5	57	3.5	57
	10, He	75	345	3.0	63	30	630
250	1, Ar	105	245	0.5	36	0.5	36
	1, He	68	295	4.0	55	4.0	55
	10, He	77	365	4.0	60	40	600
300	1, Ar	108	245	0.2	40	0.2	40
	1, He	73	315	3.5	54	3.5	54
	10, He	91	380	3.5	59	35	590
350	1, Ar	115	245	0.1	47	0.1	47
	1, He	75	305	2.0	52	2.0	52
	10, He	98	375	2.0	56	20	560

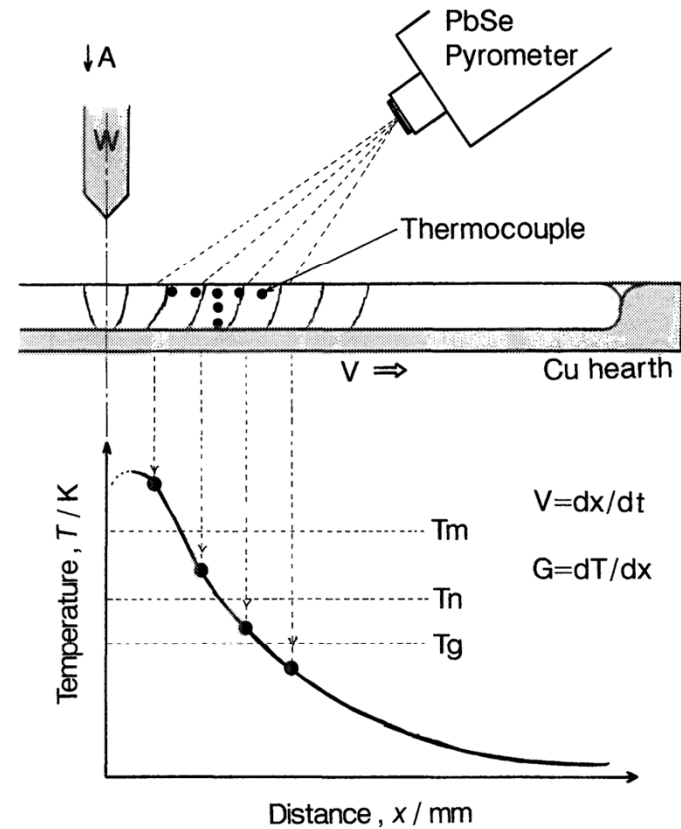


Fig. 1 Schematic illustration of the method to measure the solidification parameters of the moving velocity of the liquid/solid interface ( $V = dx/dt$ ) and temperature gradient ( $G = dT/dx$ ) in a unidirectional arc melting technique.

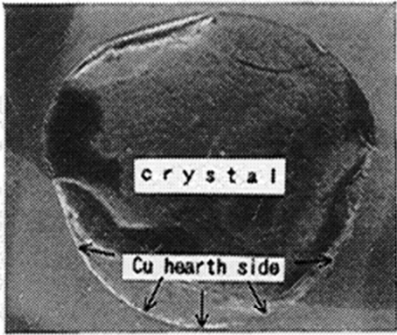
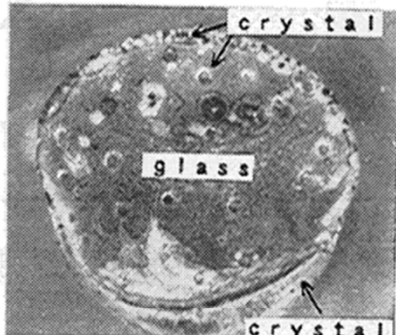
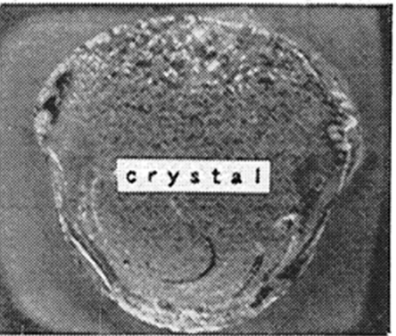
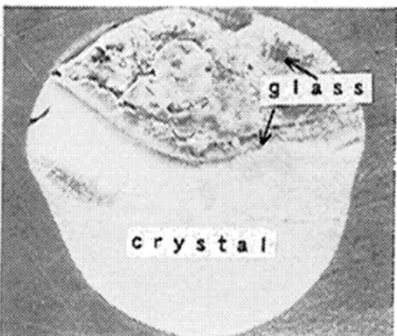
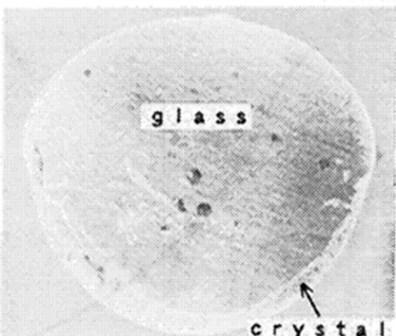
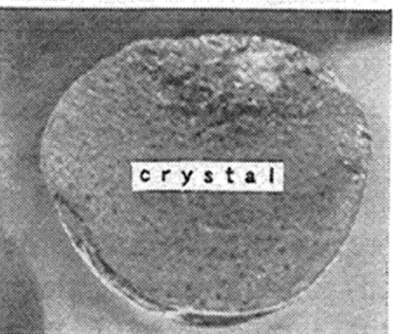
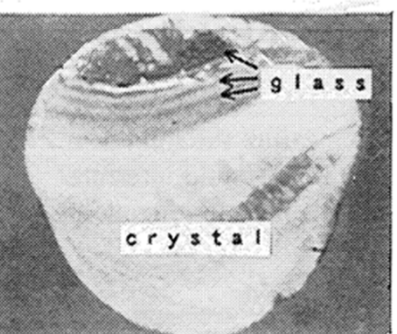
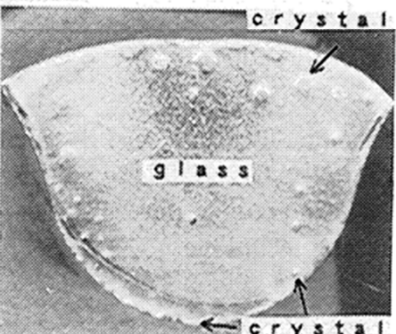
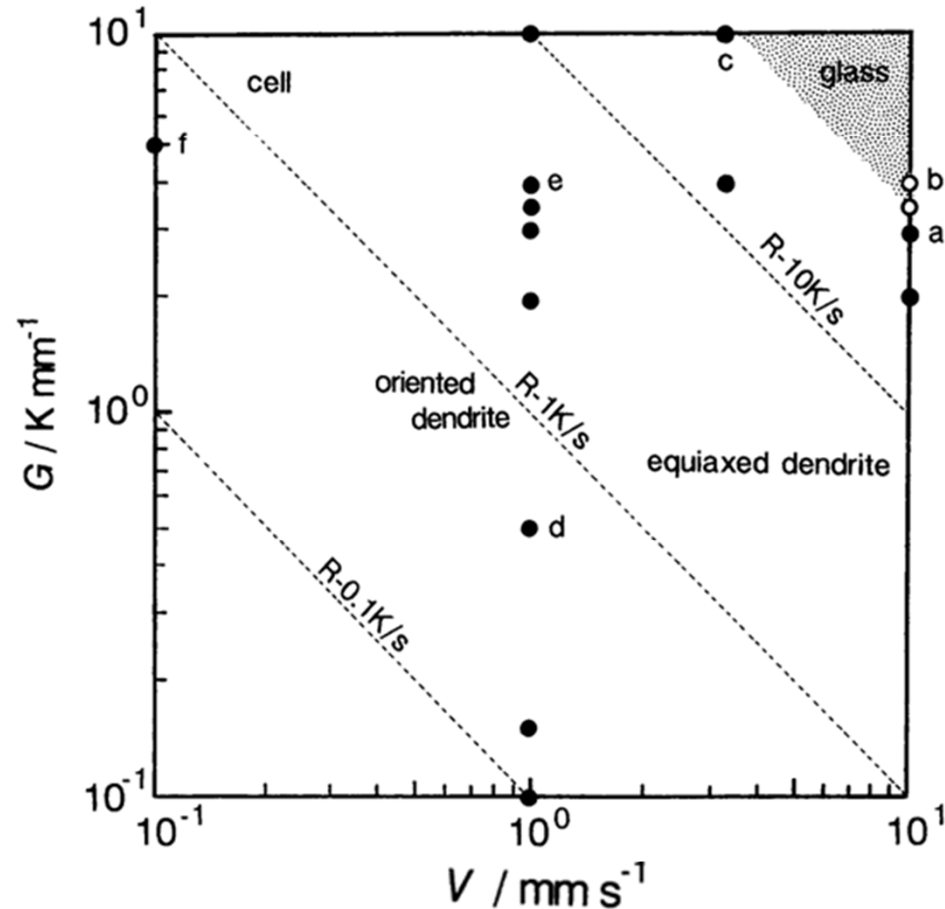
A \ gas V	Ar , 1 mm/s	He , 1 mm/s	He , 10 mm/s
250			
300			
350			

Fig. 3 Relation among the transverse cross sectional structure, arc current, moving velocity of liquid/solid interface and flowing gas for the unidirectionally arc-melted  $Zr_{60}Al_{10}Ni_{10}Cu_{15}Pd_5$  ingots.

Fig. 4 Relation among the solidification structure, the moving velocity of liquid/solid interface ( $V$ ), temperature gradient ( $G$ ) and cooling rate ( $R=V\times G$ ) for the unidirectionally arc-melted  $Zr_{60}Al_{10}Ni_{10}Cu_{15}Pd_5$  ingots. The closed and open circles represent the experimental points where crystalline and glassy phases are formed, respectively.



$R_c$ : 40 K/s

- Critical cooling rate is not a absolute physical value.
- It is a variable value by preliminary treatment of the molten alloy before vitrification.

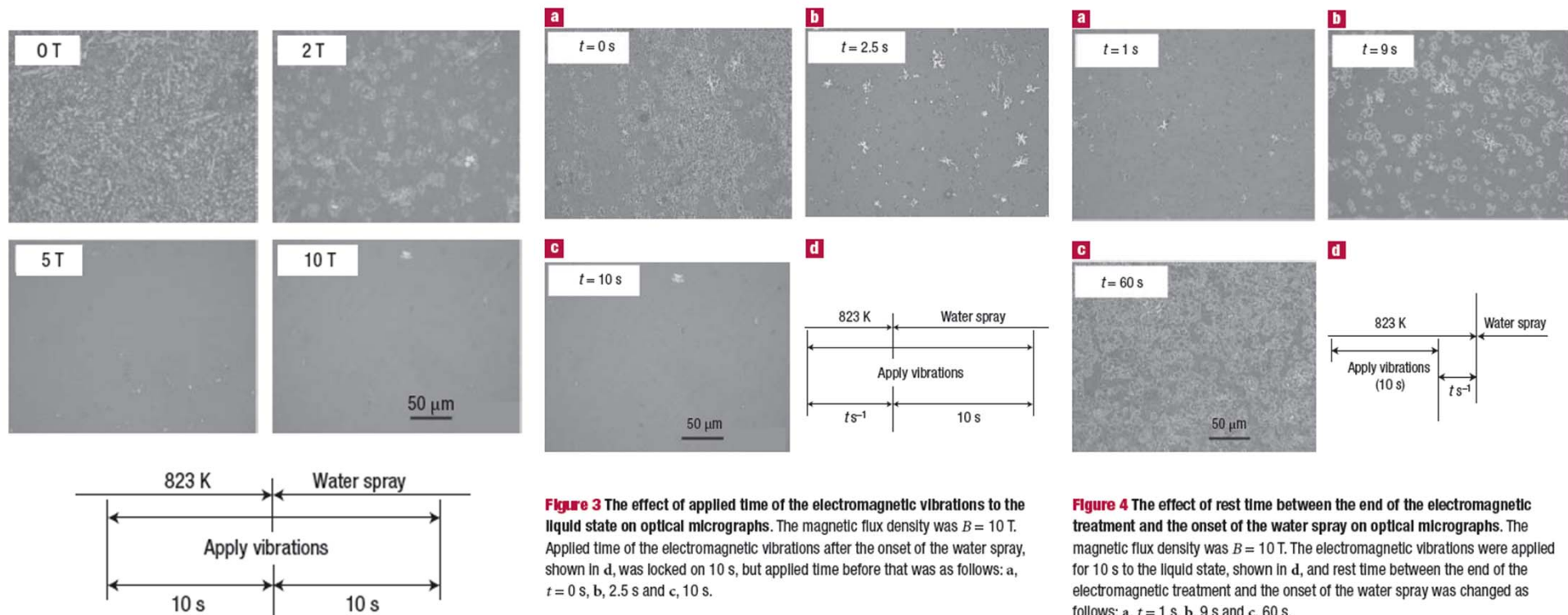
## 4.6 Bulk Metallic Glass Casting Methods

### 4.6.9 Electromagnetic Vibration Process

: Electromagnetic and stationary magnetic fields could act as powerful vibrating forces in the melt → destroy clusters of strong local order and consequently eliminates the opportunity for the crystalline phases to nucleate → GFA↑

- Increasing the magnitude of the magnetic flux density and/or applying these vibrations for longer time helps in the destruction of these clusters. On the other hand, by increasing the rest time between melting and water spraying, the molten alloy is having enough time to reform the clusters, and therefore the GFA of the alloy is decreased. → need to control the process parameters

nature **materials** | VOL 4 | APRIL 2005 |



## 4.6 Bulk Metallic Glass Casting Methods

### 4.8 Mechanical Alloying

: another popular technique to synthesize amorphous phases in a number of alloy system

[Cons] Multi-step process

→ need to be consolidated in SCLR by some of conventional or innovative methods through application of pressure and/or temperature

[Pros] wide composition ranges

→ used to easily produce amorphous phases in those systems where conventional melting and casting methods prove difficult or impossible

→ Combination of small particle size, reduced diffusion distances across the lamellar structure, fresh surfaces and interfaces, coupled with a slight rise in temperature → increased atomic diffusivity and therefore alloying occurs

→ Kinetics of microstructural refinement:  
depends on the mechanical properties of the powder, type of the milling used, ball-to-powder weight ratio, and the milling temperature

Grinding Medium (stainless steel or Tungsten carbide or other hard mater.)  
: subjected to shear, impact, or other type of mechanical force

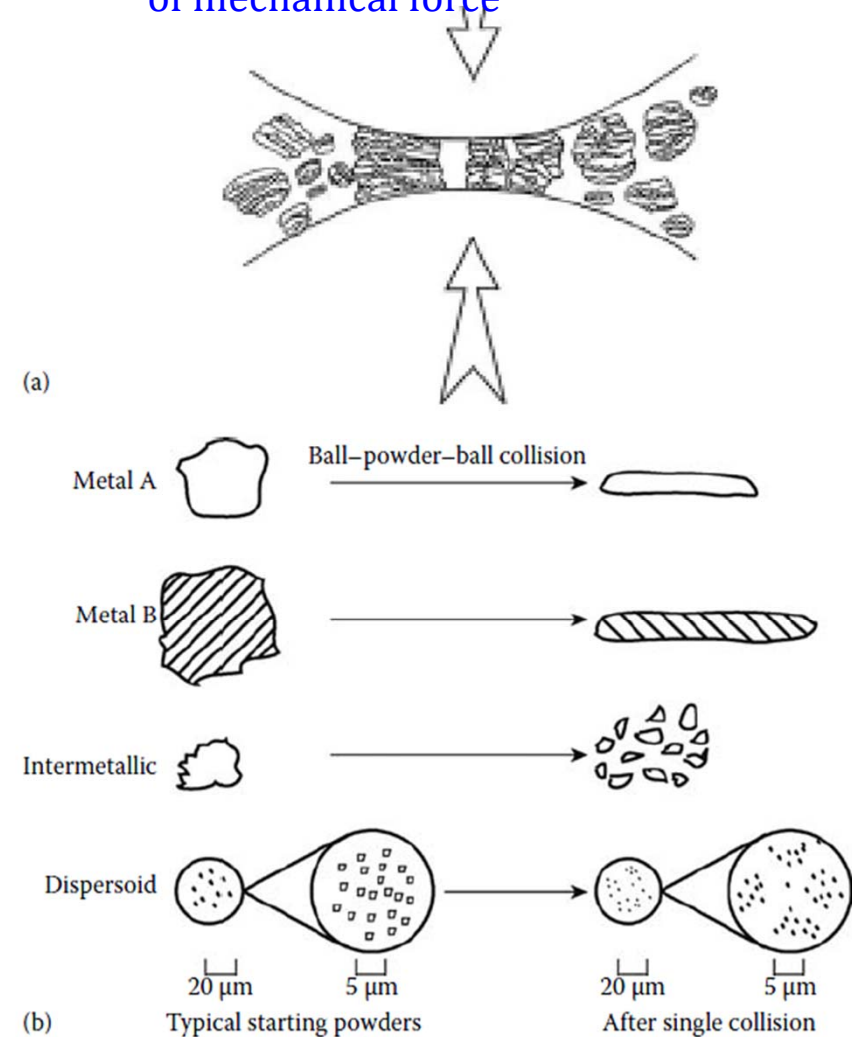


FIGURE 4.15

(a) Ball-powder-ball collision of powder mixture during MA and (b) deformation characteristics of representative constituents of starting powders in MA. Note that the ductile metal powders (metals A and B) get flattened, while the brittle intermetallic and dispersoid particles get fragmented into smaller particles.



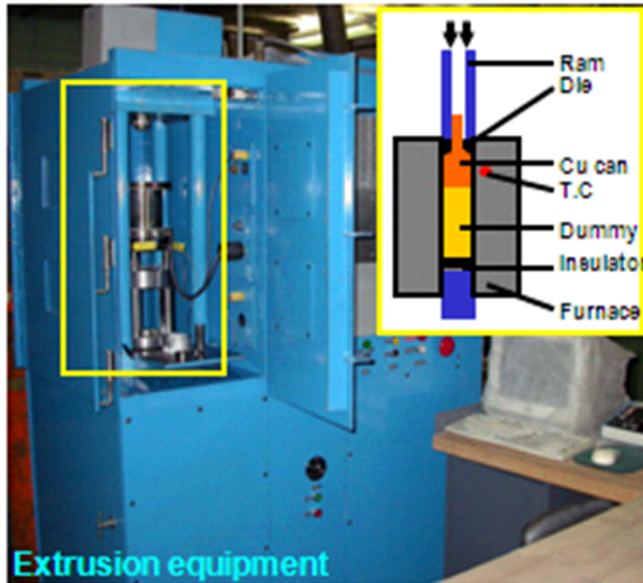
TABLE 4.3

Some Selected BMG Alloy Compositions Produced in a Glassy Condition by MA

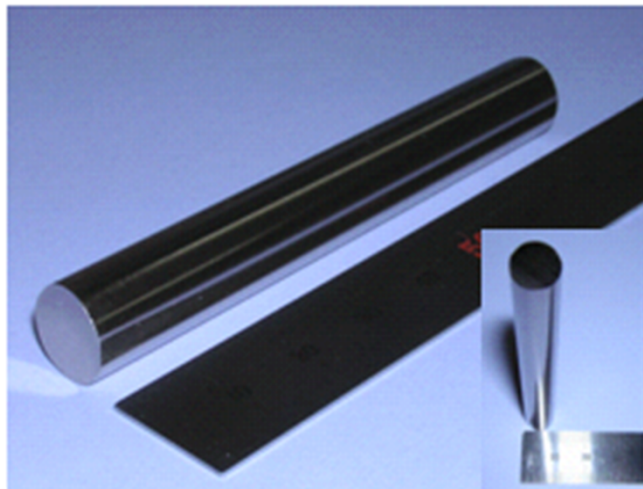
Alloy Composition	Mill	BPR	Time for Amorphization (h)	Reference
$\text{Fe}_{72}\text{Al}_5\text{Ga}_2\text{C}_6\text{B}_4\text{P}_{10}\text{Si}_1$	Planetary ball mill AGO-2U	10:1 or 20:1	8–12	[78]
$\text{Fe}_{60}\text{Co}_8\text{Zr}_{10}\text{Mo}_5\text{W}_2\text{B}_{15}$	SPEX mill	10:1	20	[79]
$\text{Fe}_{42}\text{Ge}_{28}\text{Zr}_{10}\text{B}_{20}$	SPEX mill	10:1	10	[80]
$\text{Fe}_{42}\text{Ge}_{28}\text{Zr}_{10}\text{C}_{10}\text{B}_{20}$	SPEX mill	10:1	8	[80]
$\text{Mg}_{65}\text{Cu}_{20}\text{Y}_{10}\text{Ag}_5 + \text{ZrO}_2$	Planetary mill	—	—	[81]
$\text{Nb}_{50}\text{Zr}_{10}\text{Al}_{10}\text{Ni}_{10}\text{Cu}_{20}$	Fritsch P5	14:1	200	[82]
$\text{Ta}_{55}\text{Zr}_{10}\text{Ni}_{10}\text{Al}_{10}\text{Cu}_{15}$	Tumbler mill	25:1	300	[83]
$\text{Ti}_{60}\text{Al}_{15}\text{Cu}_{10}\text{W}_{10}\text{Ni}_5$	Tumbler mill	30:1	200	[84]
$\text{V}_{45}\text{Zr}_{20}\text{Ni}_{20}\text{Cu}_{10}\text{Al}_{2.5}\text{Pd}_{2.5}$	Tumbler mill	25:1	200	[85]
$\text{Zr}_{52}\text{Al}_6\text{Ni}_8\text{Cu}_{14}\text{W}_{20}$	Tumbler mill	60:1	200	[86]

# Powder → bulk metallic glasses

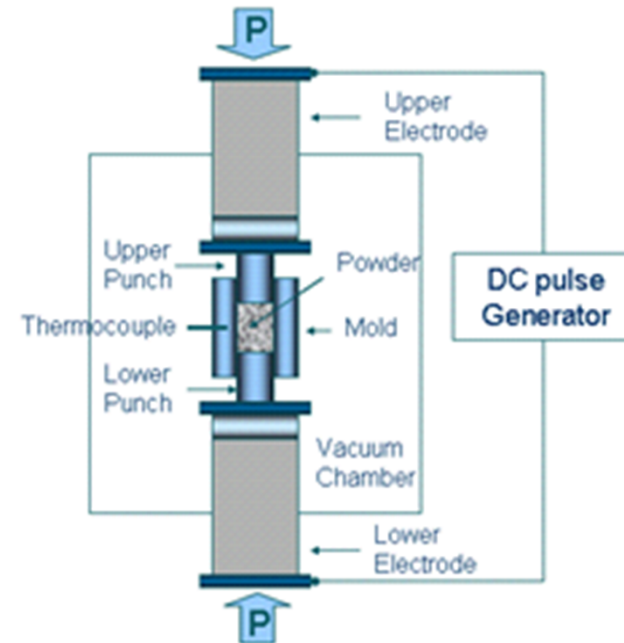
## 1) Extrusion



Extrusion equipment



## 2) Spark Plasma Sintering



Temp: 843 K  
Time: 60 s  
Load: 280 MPa

